mathematics

Article

A Refined Closed-Form Solution for the Large Deflections of Alekseev-Type Annular Membranes Subjected to Uniformly Distributed Transverse Loads: Simultaneous Improvement of Out-of-Plane Equilibrium Equation and Geometric Equation

Bo Li [1], Qi Zhang [1], Xue Li [1], Xiao-Ting He [1,2] and Jun-Yi Sun [1,2,*]

[1] School of Civil Engineering, Chongqing University, Chongqing 400045, China; 202116131339@cqu.edu.cn (B.L.); 202016021045@cqu.edu.cn (Q.Z.); 20161602025t@cqu.edu.cn (X.L.); hexiaoting@cqu.edu.cn (X.-T.H.)
[2] Key Laboratory of New Technology for Construction of Cities in Mountain Area (Chongqing University), Ministry of Education, Chongqing 400045, China
* Correspondence: sunjunyi@cqu.edu.cn; Tel.: +86-(0)23-65120720

check for updates

Citation: Li, B.; Zhang, Q.; Li, X.; He, X.-T.; Sun, J.-Y. A Refined Closed-Form Solution for the Large Deflections of Alekseev-Type Annular Membranes Subjected to Uniformly Distributed Transverse Loads: Simultaneous Improvement of Out-of-Plane Equilibrium Equation and Geometric Equation. *Mathematics* **2022**, *10*, 2121. https://doi.org/10.3390/math10122121

Academic Editors: Araceli Queiruga-Dios, Maria Jesus Santos, Fatih Yilmaz, Deolinda M. L. Dias Rasteiro, Jesús Martín Vaquero and Víctor Gayoso Martínez

Received: 7 May 2022
Accepted: 14 June 2022
Published: 17 June 2022

Abstract: The Alekseev-type annular membranes here refer to annular membranes fixed at outer edges and connected with a movable, weightless, stiff, con-centric, circular thin plate at inner edges, which were proposed originally by Alekseev for bearing centrally concentrated loads. They are used to bear the pressure acting on both membranes and plates, which was proposed originally in our previous work for developing pressure sensors. The pressure is applied onto an Alekseev-type annular membrane, resulting in the parallel movement of the circular thin plate. Such a movement can be used to develop a capacitive pressure sensor using the circular thin plate as a movable electrode plate of a parallel plate capacitor. The pressure applied can be determined by measuring the change in capacitance of the parallel plate capacitor, based on the closed-form solution for the elastic behavior of Alekseev-type annular membranes. However, the previous closed-form solution is unsuitable for annular membranes with too large deflection, which limits the range of pressure operation of the developed sensors. A new and more refined closed-form solution is presented here by improving simultaneously the out-of-plane equilibrium equation and geometric equation, making it possible to develop capacitive pressure sensors with a wide range of pressure operations. The new closed-form solution is numerically discussed in its convergence and effectiveness and compared with the previous one. Additionally, its beneficial effect on developing the proposed capacitive pressure sensors is illustrated.

Keywords: annular membrane; uniform transverse loading; large deflection; power series method; closed-form solution

MSC: 74G10; 74K15

1. Introduction

Membrane structures can be used in civil engineering, aerospace engineering, technical applications and other fields, among which, axisymmetric membrane structures are often preferred for some technical applications, such as the bulge tests [1–3], blister tests [4–6] or constrained blister tests [7–10], and non-contact or contact capacitive pressure sensors [11–14]. The problem of axisymmetric deformation of membranes in these technical applications often has strong nonlinearity due to the concomitant of large deflection. So, analytical solutions to these membrane problems are available only in a few cases, and there are far fewer analytical solutions in the literature for annular membrane problems than for circular membrane problems. However, analytical solutions are often found to be necessary to implement these technical applications. This paper is devoted to the analytical study to the problem of axisymmetric deformation with large deflection of the Alekseev-type annular membrane structures under uniformly distributed transverse loads. The analytical solution of this problem can be used to develop a kind of capacitive pressure sensor [15], but the available analytical solution in the existing literature is not suitable for the case where the annular membranes exhibit too large deflection or rotation angle [15], which limits the range of pressure operation of the developed sensors. The purpose or significance of this work is to provide a new and more refined closed-form solution for developing capacitive pressure sensors with a wide range of pressure operation.

There are two methods for analytically solving the problem of axisymmetric deformation of circular or annular membranes in the existing literature—one is the power series solution, and the other is the algebraic solution. Hencky is the first person who used the power series method to solve circular membrane problems. He presented a power series solution of a circular membrane fixed at its outer edge and loaded transversely and uniformly in 1915 [16], where a computational error was corrected, respectively, by Chien in 1948 [17] and Alekseev in 1953 [18]. This is the first solution of circular membrane problems. This solution is often referred to as the well-known Hencky's solution and is cited in related studies [19–22]. Sun et al. improved the well-known Hencky's solution many times to make it suitable for heavily loaded membranes [23]. The peripherally fixed and uniformly normally loaded circular membranes are another type of circular membrane problems [24,25], where the direction of normally loading is always perpendicular to the membrane with deflection (while the direction of transversely loading is always perpendicular to the membrane without deflection). Gas pressure is typical normal loading while structural dead weight is typical transverse loading.

According to the Mathematics Subject Classification (MSC), membranes and thin films belong to different categories in the mechanics of deformable solids of the MSC database. A membrane is not necessarily as thin as a thin film, and can be a thin film, a thin plate or even a thick plate, but must have rigid edges that do not produce displacement under transverse loads. Annular membrane problems are often more complicated than circular membrane problems because circular membranes have only outer edges while annular membranes have both outer edges and inner edges. The outer edges of annular membranes are all fixed and, thus, rigid, just like that of circular membranes, while their inner edges are all movable rigid edges, which can be divided into two types. The first type is the inner edges attached to a weightless, stiff, concentric, circular thin plate, which is proposed originally by Alekseev [26]; while the second type is those attached to a weightless stiff ring, which is proposed originally by Sun et al. [27]. For convenience, the annular membranes with the first type of inner edges are referred to simply as Alekseev-type annular membranes (or annular membrane structures) [15,26], and those with the second type of inner edges are referred to simply as Sun-type annular membranes (or annular membrane structures) [27]. In this study, only the Alekseev-type annular membranes are involved.

Alekseev is the first person to deal with annular membrane problems [26], who algebraically solved the axisymmetric deformation problem of a peripherally fixed annular membrane, connected with a movable, weightless, stiff, concentric, circular thin plate at its inner edge, and transversely loaded at the center point of the circular thin plate. However, the closed-form solution presented in [26] is valid only for membranes with Poisson's ratios less than $1/3$. Sun et al. [28] algebraically solved the problem dealt with originally by Alekseev [26] again and presented a global or complete closed-form solution that is valid for membranes with Poisson's ratio less than, equal to, or greater than $1/3$. Yang et al. [29] extended the closed-form solution presented by Sun et al. [28] to the more general case of annular membranes with or without initial in-plane stress. In fact, many widely used thin films, such as polymers, often have Poisson's ratios greater than $1/3$, and all the structures constituted more or less have some initial in-plane stresses. It is worth mentioning that the solutions presented by Alekseev [26], Sun et al. [28] and Yang et al. [29] are the only three algebraic solutions for membrane problems in the literature so far, which are derived from directly solving nonlinear differential equations by the algebraic method. As mentioned above, all these three solutions apply only to the problem of axisymmetric deformation of Alekseev-type annular membrane structures under concentrated forces, the case where the external loads (the concentrated forces) are applied at the center point of the weightless, stiff, concentric, circular thin plates and do not directly contact the annular membranes.

Lian et al. [15] proposed to use Alekseev-type annular membrane structures to design a membrane elastic deflection and parallel plate capacitor-based capacitive pressure sensor, where the uniformly distributed transverse loads are synchronously applied onto both the weightless, stiff, concentric, circular thin plate and the annular membrane, resulting in the parallel movement of the circular thin plate. It is obvious that the distance of parallel movement of the circular thin plate, wich is caused by the application of uniformly distributed transverse loads, is exactly equal to the maximum deflection of the annular membrane. Therefore, the circular thin plate, if made of conductive materials, can be used as a movable electrode plate of a parallel plate capacitor. The change in the capacitance of the parallel plate capacitor corresponds to the distance of parallel movement of the circular thin plate, also the maximum deflection of the annular membrane, and the uniformly distributed transverse loads applied. In this way, the pressure applied, i.e., the applied uniformly distributed transverse loads, may be determined by measuring the capacitance of the parallel plate capacitor, as long as the closed-form solution of the axisymmetric elastic deformation of the Alekseev-type annular membrane under uniformly distributed transverse loads can be obtained. Such a closed-form solution has been given by Lian et al. [15], which is in the form of power series. This closed-form solution is also the first power series solution for annular membrane problems. The derivation of this power series solution was a salutary reminder of the convergence of annular membrane problems: the power series method for annular membrane problems is more difficult to converge than that for circular membrane problems, due to the fact that the stress, strain or deflection in annular membrane problems can not be expanded into a power series at the center of the membranes while that in circular membrane problems can. This limitation means that the annular membrane problems solved by using the power series method must be first examined in convergence before the convergence of their power series solutions can be tested.

However, the closed-form solution presented by Lian et al. [15] is not applicable to the case where the annular membranes exhibit a too large rotation angle or deflection, because it was derived from the assumption of a small rotation angle of membrane which is usually adopted in membrane problems. This assumption will affect the accuracy of the closed-form solution and introduce large computational errors, especially when heavily loaded membranes exhibit a large rotation angle or deflection. In the derivation of the closed-form solution presented by Lian et al. [15], the out-of-plane and in-plane equations and geometric equations are established by using the assumption of a small rotation angle, except that the physical equations are established by using the assumption of a small deformation (the stress–strain relationships are assumed to satisfy Hooke's law). In this paper, the physical equations are still assumed to satisfy Hooke's law, but the assumption of a small rotation angle of membrane is given up during the establishments of the out-of-plane equilibrium equation and geometric equations, resulting in a new and more refined closed-form solution. Furthermore, our attempt to simultaneously give up the assumption of a small rotation angle in the establishments of the geometric equation, in-plane equation and out-of-plane equilibrium equation failed to achieve a closed-form solution. This suggests, to some extent, that the power series method for annular membrane problems is much more complicated than the power series method for circular membrane problems.

The paper is organized as follows: The problem of axisymmetric deformation with large deflection of an Alekseev-type annular membrane under uniformly distributed transverse loads is reformulated and solved in the following section, where the out-of-plane equilibrium equation and geometric equations are re-established with the assumption of a small rotation angle of membrane given up, and finally, a new and more refined closed-form solution of the problem under consideration is given. In Section 3, the convergence and effectiveness of the closed-form solution given in Section 2 are discussed. A numerical comparison between the present and previous closed-form solutions was conducted. The beneficial effect of the improved closed-form solution in Section 2 on developing the capacitive pressure sensors proposed by Lian et al. [15] is investigated by comparing the pressure values, which are, under the same deflection, calculated by using the closed-form solution presented in this paper and using the one presented by Lian et al. [15]. Concluding remarks are given in Section 4.

The innovation of this paper is mainly reflected in the following two aspects: one is the contribution to thin film mechanics, and the other is the practical applications that can be derived from this study. The new closed-form solution derived in Section 2 can be used for heavily loaded annular membranes with larger rotation angles, while the previous closed-form solution is only suitable for lightly loaded annular membranes with smaller rotation angles, thus, developing and enriching the theory of annular membranes. On the other hand, by simultaneously improving the out-of-plane equilibrium equation and geometric equation, the computational accuracy of the new closed-form solution is greatly improved. Therefore, if the new closed-form solution is used to design the capacitive pressure sensors proposed by Lian et al. [15], the pressure measurement error of the sensors designed may be reduced by up to 40% in comparison with the use of the previous closed-form solution, which is also the application significance and value of the work presented here.

2. Membrane Equation and Its Solution

A linearly elastic, initially flat annular membrane with inner radius b, outer radius a, thickness h, Young's modulus of elasticity E and Poisson's ratio v is fixed at its outer edge and connected at its inner edge with a movable, concentric, weightless, stiff, circular thin plate, forming an Alekseev-type annular membrane structure. A loads q is uniformly, transversely and quasi-statically applied onto the circular thin plate and the annular membrane, resulting in an out-of-plane displacement (deflection) of the annular membrane and a parallel movement of the circular thin plate, as shown in Figure 1, where the origin o of the introduced cylindrical coordinate system (r, φ, w) sits at the centroid of the initially flat annular membrane, the geometric middle plane of the initially flat annular membrane is located in the polar coordinate plane (r, φ), the radial coordinate is denoted by r, the angle coordinate is denoted by φ but not shown in Figure 1, and the axial coordinate is denoted by w that also denotes the deflection of the deflected annular membrane. Suppose a free body of a deflected annular membrane of radius r ($b \le r \le a$) is taken from the central portion of the deflected annular membrane, to study the static equilibrium of this free body under the joint action of the external active force $\pi r^2 q$ and internal reactive force $2\pi r \sigma_r h$, which are produced by the uniformly distributed transverse loads q and the membrane force $\sigma_r h$ at the boundary r, as shown in Figure 2, where θ is the rotation angle of the deflected annular membrane and σ_r is the radial stress.

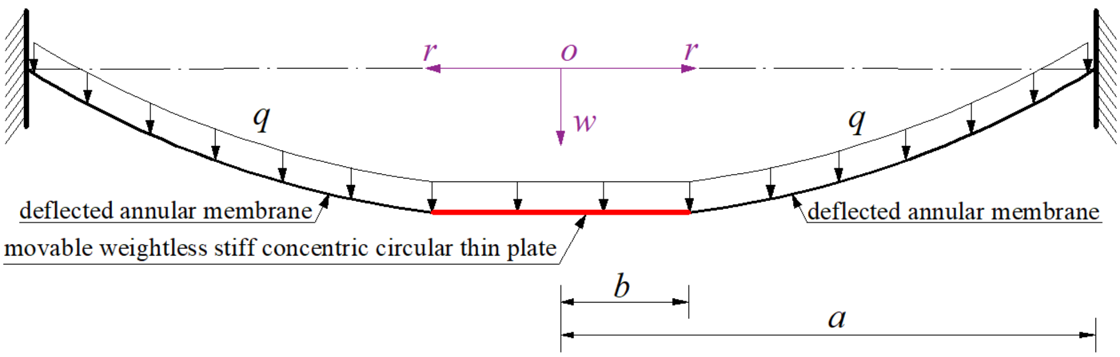

Figure 1. Deflection profile along a diameter of an Alekseev-type annular membrane under loads q.

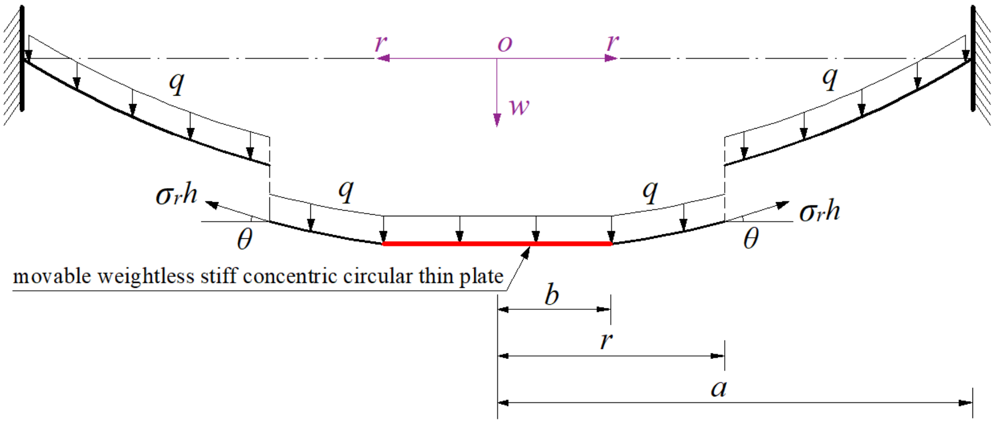

Figure 2. Equilibrium diagram of the free body with radius r ($b \le r \le a$).

In the transverse (vertical) direction, there are only two opposing forces, i.e., $\pi r^2 q$ and $2\pi r\sigma_r h\sin\theta$. Therefore, the equilibrium condition in this direction is that the resultant force of these two opposing forces is equal to zero, i.e.,

$$\pi r^2 q - 2\pi r\sigma_r h\sin\theta = 0. \tag{1}$$

If $w(r)$ is used to denote the deflection of the annular membrane at r, then

$$\tan\theta = -\frac{\mathrm{d}w(r)}{\mathrm{d}r}. \tag{2}$$

It is well known from trigonometric functions that $\sin\theta = 1/\sqrt{1+1/\tan^2\theta}$. Therefore, from Equations (1) and (2), the so-called out-of-plane equilibrium equation can be written as

$$2\sigma_r h = rq\sqrt{1+1/(-\mathrm{d}w/\mathrm{d}r)^2}. \tag{3}$$

By comparing Equation (3) in this paper and Equation (4) in [15], it can be found that the out-of-plane equilibrium equation in [15], i.e., Equation (4) in [15], uses the assumption of $\sin\theta = \tan\theta$. Obviously, this assumption is valid only when the rotation angle of membrane, θ, is small. For instance, the error caused by the assumption of $\sin\theta = \tan\theta$ can be written as $(\tan\theta - \sin\theta)/\sin\theta$ and is about 1.54% when $\theta = 10°$, 6.42% when $\theta = 20°$, 15.47% when $\theta = 30°$, and 30.54% when $\theta = 40°$. However, Equation (3) is not affected by this assumption, since this assumption is given up during the establishment of Equation (3).

If the circumferential stress is denoted by σ_t, then the in-plane equilibrium equation may be written as [15]

$$\frac{\mathrm{d}}{\mathrm{d}r}(r\sigma_r h) - \sigma_t h = 0. \tag{4}$$

If the radial displacement and strain and circumferential strain are denoted by $u(r)$, e_r and e_t, respectively, then the geometric equations may be written as [23]

$$e_r = \left[\left(1+\frac{\mathrm{d}u}{\mathrm{d}r}\right)^2 + \left(\frac{\mathrm{d}w}{\mathrm{d}r}\right)^2\right]^{1/2} - 1 \tag{5}$$

and

$$e_t = \frac{u}{r} \tag{6}$$

By comparing Equation (5) in this paper and Equation (6a) in [15], it can be found that the radial relationship between strain and displacement has been changed. The classical radial relationship between strain and displacement, i.e., Equation (6a) in [15], is heavily dependent on the assumption of small rotation angle of membrane, see [23] for details.

Moreover, the physical equations are still assumed to be linearly elastic [15]

$$\sigma_r = \frac{E}{1-\nu^2}(e_r + \nu e_t) \tag{7}$$

and

$$\sigma_t = \frac{E}{1-\nu^2}(e_t + \nu e_r). \tag{8}$$

In the above physical equations, geometric equations, in-plane equilibrium equation and out-of-plane equilibrium equation, there are six equations and six variables, i.e., σ_r, σ_t, e_r, e_t, $u(r)$ and $w(r)$. Therefore, this boundary value problem can be solved. Substituting Equations (5) and (6) into Equations (7) and (8) yields

$$\sigma_r = \frac{E}{1-\nu^2}\{[(1+\frac{\mathrm{d}u}{\mathrm{d}r})^2 + (\frac{\mathrm{d}w}{\mathrm{d}r})^2]^{1/2} - 1 + \nu\frac{u}{r}\} \tag{9}$$

and

$$\sigma_t = \frac{E}{1-\nu^2}\{\frac{u}{r} + \nu[(1+\frac{\mathrm{d}u}{\mathrm{d}r})^2 + (\frac{\mathrm{d}w}{\mathrm{d}r})^2]^{1/2} - \nu\}. \tag{10}$$

Eliminating *u/r* from Equations (9) and (10) and using Equation (4) yields

$$\frac{u}{r} = \frac{1}{Eh}(\sigma_t h - \nu\sigma_r h) = \frac{1}{Eh}[\frac{\mathrm{d}}{\mathrm{d}r}(r\sigma_r h) - \nu\sigma_r h]. \tag{11}$$

After the u in Equation (11) is substituted into Equation (9), then the so-called consistency equation can be written as

$$\frac{\nu-1}{E}\sigma_r + \frac{\nu r}{E}\frac{\mathrm{d}\sigma_r}{\mathrm{d}r} + \{[1+\frac{(1-\nu)}{E}\sigma_r + \frac{(3-\nu)r}{E}\frac{\mathrm{d}\sigma_r}{\mathrm{d}r} + \frac{r^2}{E}\frac{\mathrm{d}^2\sigma_r}{\mathrm{d}r^2}]^2 + (\frac{\mathrm{d}w}{\mathrm{d}r})^2\}^{1/2} - 1 = 0. \tag{12}$$

σ_r, σ_t and w can be obtained by solving Equations (3), (4) and (12). The boundary conditions of solving Equations (3), (4) and (12) are

$$e_t = 0\left(\frac{u}{r} = 0\right) \text{ at } r = b, \tag{13}$$

$$e_t = 0\left(\frac{u}{r} = 0\right) \text{ at } r = a \tag{14}$$

and

$$w = 0 \text{ at } r = b. \tag{15}$$

The following dimensionless variables are introduced

$$Q = \frac{aq}{Eh}, W = \frac{w}{a}, S_r = \frac{\sigma_r}{E}, S_t = \frac{\sigma_t}{E}, \alpha = \frac{b}{a}, x = \frac{r}{a}, \tag{16}$$

and transform Equations (3), (4), (11)–(15) into

$$2S_r = xQ\sqrt{1 + 1/(-\mathrm{d}W/\mathrm{d}x)^2}, \tag{17}$$

$$\frac{\mathrm{d}(xS_r)}{\mathrm{d}x} - S_t = 0, \tag{18}$$

$$\frac{u}{r} = (1-\nu)S_r + x\frac{\mathrm{d}S_r}{\mathrm{d}x}, \tag{19}$$

$$(\nu-1)S_r + \nu x\frac{\mathrm{d}S_r}{\mathrm{d}x} + \{[1+(1-\nu)S_r + (3-\nu)x\frac{\mathrm{d}S_r}{\mathrm{d}x} + x^2\frac{\mathrm{d}^2S_r}{\mathrm{d}x^2}]^2 + (\frac{\mathrm{d}W}{\mathrm{d}x})^2\}^{1/2} - 1 = 0, \tag{20}$$

$$(1-\nu)S_r + x\frac{\mathrm{d}S_r}{\mathrm{d}x} = 0 \text{ at } x = \alpha, \tag{21}$$

$$(1-\nu)S_r + x\frac{\mathrm{d}S_r}{\mathrm{d}x} = 0 \text{ at } x = 1 \tag{22}$$

and

$$W = 0 \text{ at } x = 1. \tag{23}$$

For practical physical problems, the displacement, strain and stress are all finite within $\alpha \leq x \leq 1$. Therefore, S_r and W can be expanded into the power series of the $x - \beta$

$$S_r = \sum_{i=0}^{\infty} c_i (x-\beta)^i \tag{24}$$

and

$$W = \sum_{i=0}^{\infty} d_i (x-\beta)^i, \tag{25}$$

where $\beta = (1 + \alpha)/2$. After introducing $X = x - \beta$, then Equations (17), (20), (24) and (25) can be transformed into

$$[4S_r^2 - (X+\beta)^2 Q^2](-\frac{\mathrm{d}W}{\mathrm{d}X})^2 - (X+\beta)^2 Q^2 = 0, \tag{26}$$

$$\begin{aligned} &[1 + (1-\nu)S_r + (3-\nu)(X+\beta)\frac{\mathrm{d}S_r}{\mathrm{d}X} + (X+\beta)^2 \frac{\mathrm{d}^2 S_r}{\mathrm{d}X^2}]^2 + (\frac{\mathrm{d}W}{\mathrm{d}X})^2 \\ &-[1 - (\nu-1)S_r - \nu(X+\beta)\frac{\mathrm{d}S_r}{\mathrm{d}X}]^2 = 0 \end{aligned}, \tag{27}$$

$$S_r = \sum_{i=0}^{\infty} c_i X^i \tag{28}$$

and

$$W = \sum_{i=0}^{\infty} d_i X^i. \tag{29}$$

After substituting Equations (28) and (29) into Equations (26) and (27), the sums of the coefficients of the same powers of the X can be obtained by merging similar terms. A system of equations for determining the recursion formulas of the coefficients c_i and d_i may be obtained by letting all the sums of the coefficients be equal to zero. The resulting recursion formulas for the coefficients c_i and d_i are listed in Appendix A. It can be seen from Appendix A that the coefficients c_i (i = 2, 3, 4, ...) and d_i (i = 1, 2, 3, ...) can be expressed in terms of the first two coefficients c_0 and c_1.

The remaining coefficients c_0, c_1 and d_0 are three undetermined constants. Their values depend on the problem being dealt with, and are determined by Equations (21)–(23), the boundary conditions. After expressing the coefficients d_i (i = 1, 2, 3, ...) and c_i (i = 2, 3, 4, ...) in terms of c_0 and c_1, substituting Equation (24) into Equations (21) and (22) yields

$$(1-\nu)\sum_{i=0}^{\infty} c_i (\alpha-\beta)^i + \alpha \sum_{i=1}^{\infty} i c_i (\alpha-\beta)^{i-1} = 0 \tag{30}$$

and

$$(1-\nu)\sum_{i=0}^{\infty} c_i (1-\beta)^i + \sum_{i=1}^{\infty} i c_i (1-\beta)^{i-1} = 0, \tag{31}$$

and further, substituting Equation (25) into Equation (23) yields

$$d_0 = -\sum_{i=1}^{\infty} d_i (1-\beta)^i. \tag{32}$$

Because Equations (30) and (31) contain only c_0 and c_1, therefore, the values of c_0 and c_1 can be determined by simultaneously solving Equations (30) and (31). Further, with the known c_0 and c_1, all the values of c_i (i = 2, 3, 4, ...) and d_i (i = 1, 2, 3, ...) can be determined, and the value of d_0 can, thus, be determined by Equation (32).

Finally, with the known c_i and d_i, the particular solution of stress $\sigma_r(r)$ and deflection $w(r)$ can be determined. As for the expression of $\sigma_t(r)$, it can easily be determined with the known expression of $\sigma_r(r)$ and Equation (4). It is not necessary to address this easy problem here. Obviously, the maximum deflection, w_m, should be at $x = \alpha$, and from Equations (16) and (25), is given by

$$w_m = a\sum_{i=0}^{\infty} d_i\left(\frac{b-a}{2a}\right)^i. \tag{33}$$

From Equations (16) and (24), the maximum stress, σ_m, is given by

$$\sigma_m = \sigma_r(b) = E\sum_{i=0}^{\infty} c_i\left(\frac{b-a}{2a}\right)^i. \tag{34}$$

3. Results and Discussions

This section will first analyze the convergence of the closed-form solution given in Section 2, then investigate its effectiveness (asymptotic behavior) and, finally, make a comparison between the present and previous closed-form solutions.

3.1. Convergence Analysis

As mentioned in the introduction, the annular membrane problems solved by using the power series method are usually difficult to converge. Therefore, they must be first examined in convergence before their power series solutions are tested in convergence. To this end, an annular membrane problem is considered of an Alekseev-type annular membrane with Poisson's ratio v = 0.47, Young's modulus of elasticity E = 7.84 MPa, outer radius a = 70 mm, inner radius b = 40 mm, and thickness h = 0.2 mm subjected to the loads q = 0.0001 MPa. After the values of E, ν, a, b, h and q are substituted into Equation (16), it is found that $\alpha = 4/7$, $\beta = (1 + \alpha)/2 = 11/14$ and $Q = 0.00446429$.

First, let us truncate the infinite power series in Equations (30)–(32) to the nth terms, i.e.,

$$(1-\nu)\sum_{i=0}^{n} c_i(\alpha-\beta)^i + \alpha\sum_{i=1}^{n} ic_i(\alpha-\beta)^{i-1} = 0, \tag{35}$$

$$(1-\nu)\sum_{i=0}^{n} c_i(1-\beta)^i + \sum_{i=1}^{n} ic_i(1-\beta)^{i-1} = 0 \tag{36}$$

and

$$d_0 = -\sum_{i=1}^{n} d_i(1-\beta)^i. \tag{37}$$

The parameter n in Equations (35)–(37) can first take 2 to start the numerical calculations of the undetermined constants c_0, c_1 and d_0, then take 3, 4, . . . until 11. The results of the numerical calculations of c_0, c_1 and d_0 are listed in Table 1. The variations of c_0, c_1 and d_0 with n are shown in Figures 3–5, where the dash-dotted lines show the convergence trends of the data points of even terms (n = 2, 4, 6 . . .) and the dashed lines show that of odd terms (n = 3, 5, 7 . . .). From Figures 3–5, it can be seen that the data sequences for c_0, c_1 and d_0 have a very good convergence trend and show a very good saturation when the parameter n takes 8 or 9, which indicates that the undetermined constants c_0, c_1 and d_0 when q = 0.0001 MPa can take the numerical values calculated by n = 8 or 9.

Table 1. The results of numerical calculation of c_0, c_1 and d_0 for q = 0.0001 MPa.

n	c_0	c_1	d_0
2	0.01197985	−0.00943991	0.03886790
3	0.01492981	−0.00851534	0.03058498
4	0.01287976	−0.00753818	0.03579442
5	0.01323855	−0.00739810	0.03468850
6	0.01301745	−0.00730386	0.03531982

Table 1. *Cont.*

n	c_0	c_1	d_0
7	0.01306394	−0.00728509	0.03517532
8	0.01303710	−0.00727377	0.03525289
9	0.01304256	−0.00727152	0.03523588
10	0.01303968	−0.00727034	0.03524527
11	0.01304025	−0.00726945	0.03524248

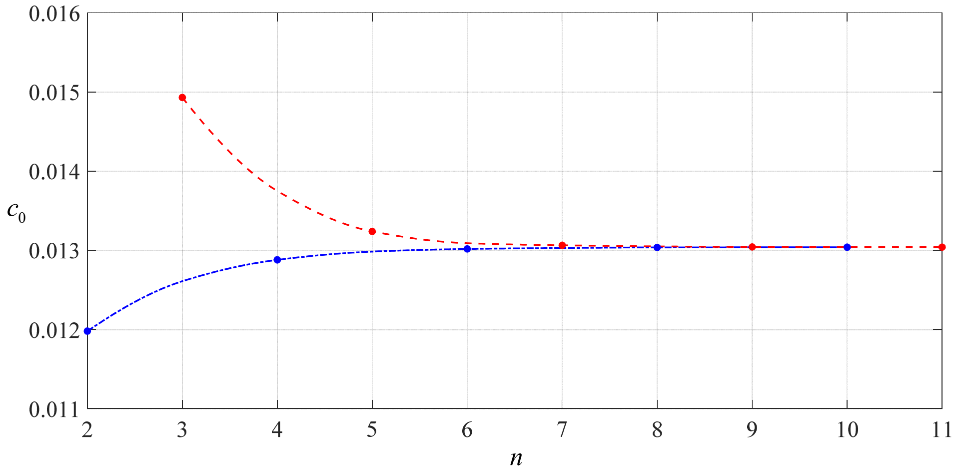

Figure 3. Variation of c_0 with n for q = 0.0001 MPa, where the dash-dotted line shows the convergence trend of the data points of even terms (n = 2, 4, 6 . . .) and the dashed line shows that of odd terms (n = 3, 5, 7 . . .).

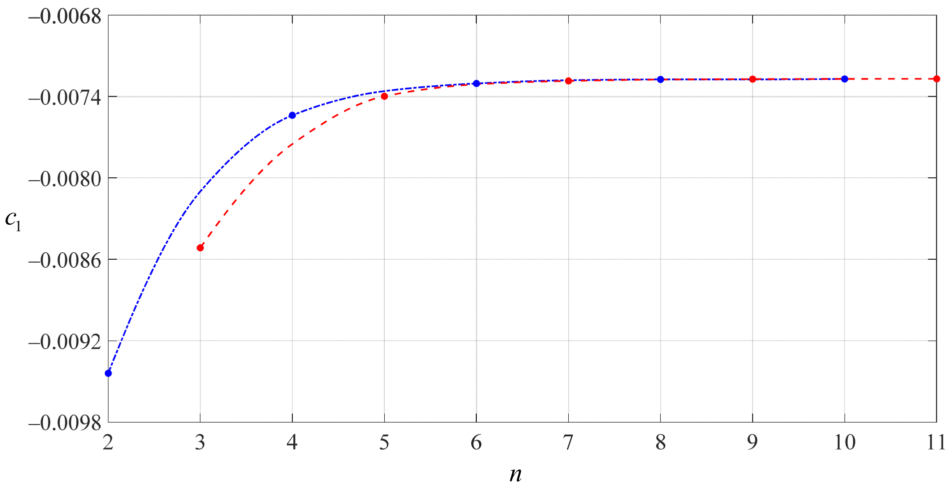

Figure 4. Variation of c_1 with n for q = 0.0001 MPa, where the dash-dotted line shows the convergence trend of the data points of even terms (n = 2, 4, 6 . . .) and the dashed line shows that of odd terms (n = 3, 5, 7 . . .).

It is well known that higher order equations can generate multiple roots, meaning, multiple roots of c_0 and c_1 could be generated when solving Equations (35) and (36) simultaneously. In boundary value problems, however, there are usually no judgment conditions that can be used to determine which of these roots is a valid root. However, it can be believed that since the power of the power series in Equations (35)–(37) is continuously increasing at equal intervals (i.e., the parameter n in Equations (35)–(37) consecutively takes values from 2 to 11), the corresponding results of numerical calculations of c_0, c_1 and d_0 should also be consecutively changing. Therefore, the variations of the numerically calculated values of c_0, c_1 and d_0 with n should obey some continuous and smooth functions, and, if expressed graphically, should follow some continuous and smooth curves. So, continuity and smoothness can be used to judge and determine valid roots, and the results of numerical calculations of c_0, c_1 and d_0 listed in Table 1 are obtained in such a way (invalid roots are not listed in Table 1). Of course, we can also make no distinction between odd and even terms when drawing Figures 3–5. This will give oscillation convergence trends, as shown in Figures 6–8. However, doing so is not conducive to the full demonstration of smoothness in some cases, as shown in Figure 7 (please compare to Figure 4).

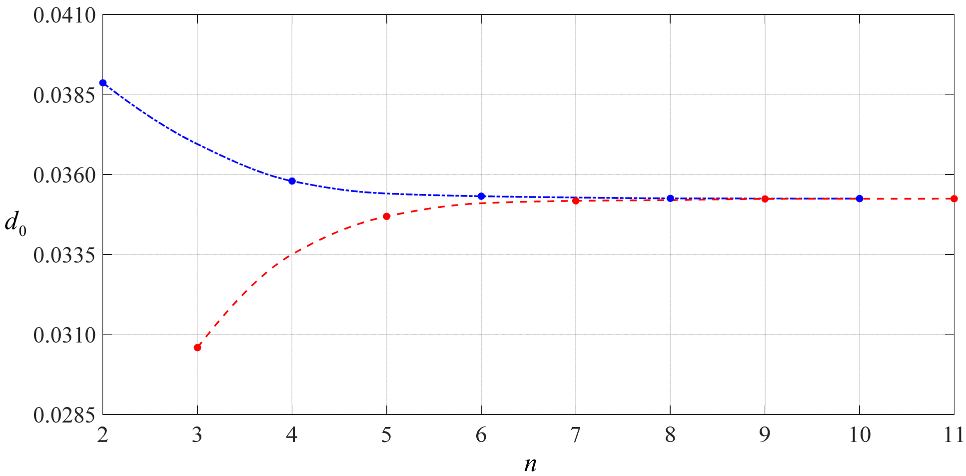

Figure 5. Variation of d_0 with n for q = 0.0001 MPa, where the dash-dotted line shows the convergence trend of the data points of even terms (n = 2, 4, 6 . . .) and the dashed line shows that of odd terms (n = 3, 5, 7 . . .).

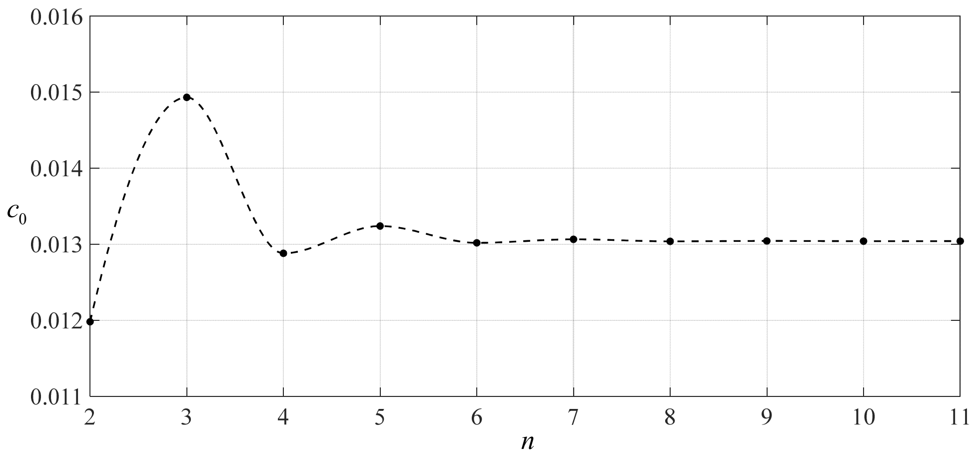

Figure 6. Variation of c_0 with n for q = 0.0001 MPa.

It should be pointed that for the boundary value problems solved by the power series method, the convergence of the particular solutions can be checked only after the convergence values of the undetermined constants $c0$, $c1$ and $d0$ are determined. From Figures 3–5 or Figures 6–8, it can be seen that the data sequences of $c0$, $c1$ and $d0$ have been converging well at about n = 8 or 9, therefore, the undetermined constants $c0$, $c1$ and $d0$ when q = 0.0001 MPa can take the numerical values calculated by $n \geq 8$ or 9. Here, we take the numerical values at n = 11 in Table 1 as the convergence values of the undetermined constants $c0$, $c1$ and $d0$ when q = 0.0001 MPa, that is, $c0$ = 0.01304025, $c1$ = $-$0.00726945 and $d0$ = 0.03524248. Obviously, the power series particular solutions of stress and deflection converge throughout the closed interval [4/7, 1] as long as they converge at the two ends of the closed interval. Tables 2 and 3 show the numerical values of stress and deflection at the two ends of the closed interval [4/7, 1], which are calculated by using Equations (24) and (25). Figures 9–12 show the variations of $ci(1-\beta)^i$,

$c_i(\alpha - \beta)^i$, $d_i(1 - \beta)^i$ and $d_i(\alpha - \beta)^i$ with i, indicating that the power series particular solutions of stress and deflection converge very quickly.

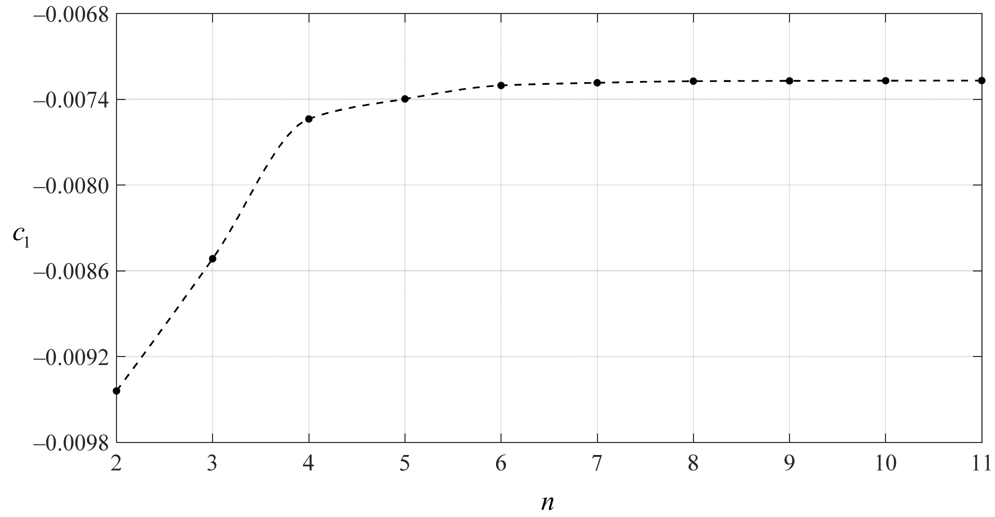

Figure 7. Variation of c_1 with n for q = 0.0001 MPa.

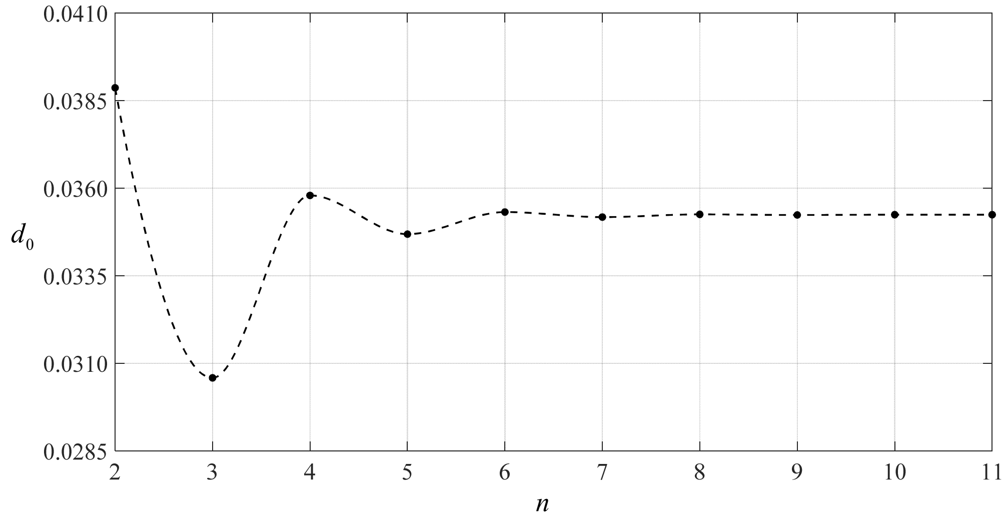

Figure 8. Variation of d_0 with n for q = 0.0001 MPa.

Table 2. The numerically calculated values of $c_i(1 - \beta)^i$ and $c_i(\alpha - \beta)^i$ when q = 0.0001 MPa, $\alpha = 4/7$ and $\beta = 11/14$.

i	$c_i(1-\beta)^i$	$c_i(\alpha-\beta)^i$
0	0.01304025	0.01304025
1	−0.00155774	0.00155774
2	0.00029641	0.00029641
3	−0.00016810	0.00016810
4	$5.29538927 \times 10^{-5}$	$5.29538927 \times 10^{-5}$
5	$-1.80161742 \times 10^{-5}$	$1.80161742 \times 10^{-5}$
6	$5.60599264 \times 10^{-6}$	$5.60599264 \times 10^{-6}$
7	$-1.75933493 \times 10^{-6}$	$1.75933493 \times 10^{-6}$
8	$5.35507803 \times 10^{-7}$	$5.35507803 \times 10^{-7}$
9	$-1.62632278 \times 10^{-7}$	$1.62632278 \times 10^{-7}$
10	$4.86626780 \times 10^{-8}$	$4.86626780 \times 10^{-8}$
11	$-1.44986110 \times 10^{-8}$	$1.44986110 \times 10^{-8}$

Table 3. The numerically calculated values of $d_i(1-\beta)^i$ and $d_i(\alpha-\beta)^i$ when q = 0.0001 MPa, α = 4/7 and β = 11/14.

i	$d_i(1-\beta)^i$	$d_i(\alpha-\beta)^i$
0	0.03524248	0.03524248
1	−0.02908424	0.02908424
2	–0.00580824	−0.00580824
3	–0.00028009	0.00028009
4	$-5.91427706 \times 10^{-5}$	$-5.91427706 \times 10^{-5}$
5	$-9.23001859 \times 10^{-6}$	$9.23001859 \times 10^{-6}$
6	$-8.68232313 \times 10^{-7}$	$-8.68232313 \times 10^{-7}$
7	$-4.31388327 \times 10^{-7}$	$4.31388327 \times 10^{-7}$
8	$-3.77046968 \times 10^{-9}$	$-3.77046968 \times 10^{-9}$
9	$-1.85145370 \times 10^{-8}$	$1.85145370 \times 10^{-8}$
10	$-1.25152469 \times 10^{-10}$	$-1.25152469 \times 10^{-10}$
11	$-5.73606617 \times 10^{-10}$	$5.73606617 \times 10^{-10}$

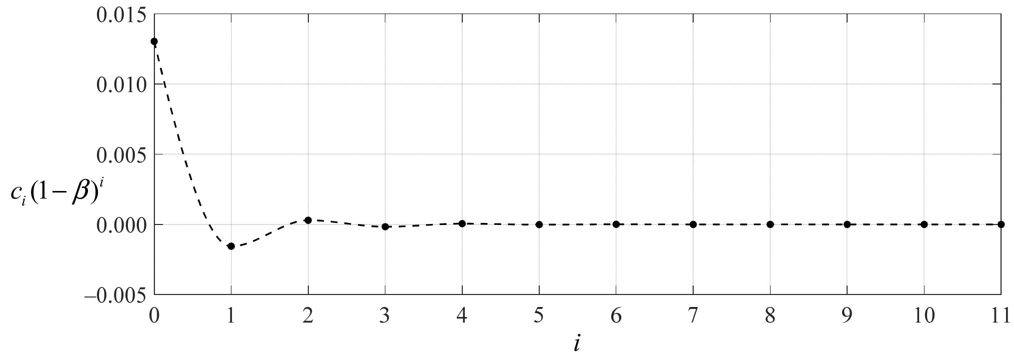

Figure 9. Variation of $c_i(1-\beta)^i$ with i for q = 0.0001 MPa and β = 11/14.

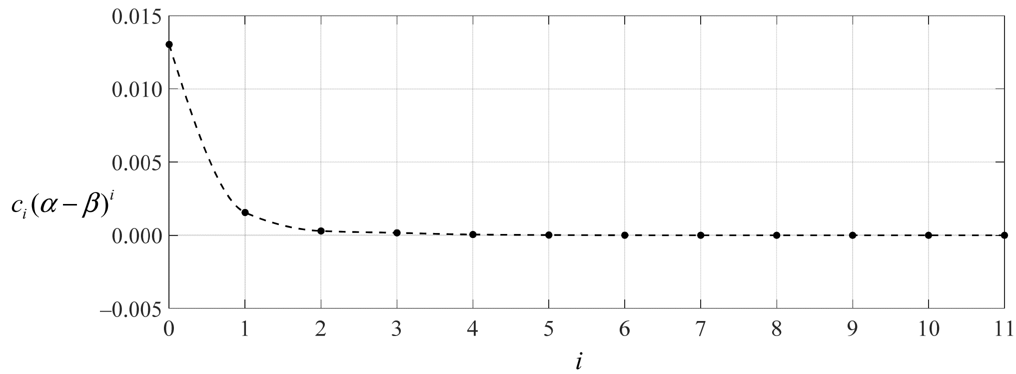

Figure 10. Variation of $c_i(\alpha-\beta)^i$ with i for q = 0.0001 MPa, α = 4/7 and β = 11/14.

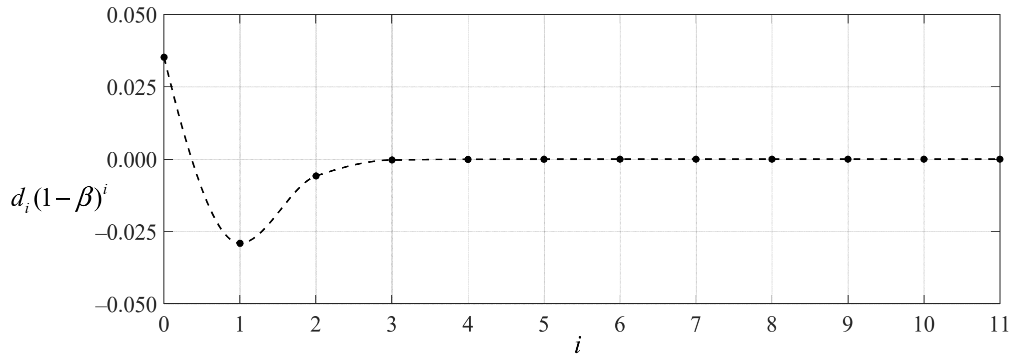

Figure 11. Variation of $d_i(1-\beta)^i$ with i for q = 0.0001 MPa and β = 11/14.

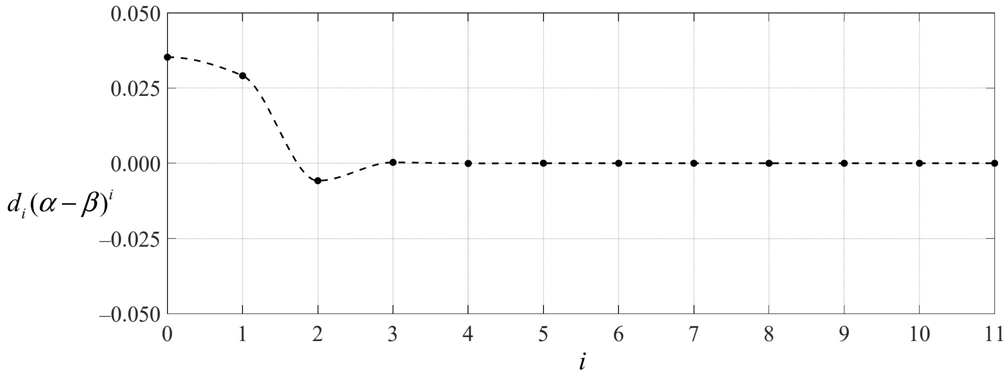

Figure 12. Variation of $d_i(\alpha-\beta)^i$ with i for q = 0.0001 MPa, $\alpha = 4/7$ and $\beta = 11/14$.

In fact, the magnitude of the applied loads q (corresponding to the different geometry of a deflected annular membrane) has a certain effect on the convergence values of the undetermined constants c_0, c_1 and d_0, which can be seen from the calculations below. Let us continue with the example above but increase the loads q from 0.0001 MPa to 0.008 MPa. Table 4 shows the results of the numerical calculation of the undetermined constants c_0, c_1 and d_0 for the problem of an Alekseev-type annular membrane with Poisson's ratio v = 0.47, Young's modulus of elasticity E = 7.84 MPa, outer radius a = 70 mm, inner radius b = 40 mm and thickness h = 0.2 mm, where q = 0.008 MPa, $\alpha = 4/7$, $\beta = (1+\alpha)/2 = 11/14$ and $Q = aq/Eh$ = 0.35714286. The variations of c_0, c_1 and d_0 with n are shown in Figures 13–15, where the dash-dotted lines show the convergence trend of the data points of even terms (n = 2, 4, 6 ...) and the dashed line show that of odd terms (n = 3, 5, 7 ...). From Figures 13–15, it can be seen that the data sequences of c_0, c_1 and d_0 have a very good convergence trend and show a very good saturation when the parameter n takes 9 or 10, which indicates that the undetermined constants c_0, c_1 and d_0 when q = 0.008 MPa can take the numerical values calculated by n = 9 or 10.

Table 4. The results of the numerical calculation of c_0, c_1 and d_0 when q = 0.008 MPa.

n	c_0	c_1	d_0
2	0.24525643	−0.19325783	0.19851576
3	0.29529305	−0.16306971	0.14895366
4	0.26747513	−0.14877045	0.17425372
5	0.27846455	−0.14657377	0.16504231
6	0.27237181	−0.14333397	0.17021351
7	0.27426590	−0.14246365	0.16824011
8	0.27364233	−0.14211856	0.16936731
9	0.27435725	−0.14198977	0.16918853
10	0.27420479	−0.14206417	0.16928792
11	0.27422132	−0.14202197	0.16921323
12	0.27421202	−0.14205290	0.16926132
13	0.27421591	−0.14203814	0.16923154

From the comparison between Figures 13–15 and Figures 3–5, it can be seen that due to the increase from q = 0.0001 MPa to q = 0.008 MPa, the convergence points have been moved slightly back, i.e., from n = 8 or 9 at q = 0.0001 MPa (see Figures 3–5) to n = 9 or 10 at q = 0.008 MPa (see Figures 13–15). This means that the magnitude of the applied loads q has a certain effect on the convergence values of the undetermined constants c_0, c_1 and d_0.

From Figures 13–15, it can be seen that the data sequences of c_0, c_1 and d_0 have been converging well at about n = 9 or 10, indicating that the undetermined constants c_0, c_1 and d_0 when q = 0.008MPa can take the numerical values calculated by $n \geq 9$ or 10. Therefore, the numerical values at n = 13 in Table 4, i.e., c_0 = 0.27421591, c_1 = −0.14203814 and d_0 = 0.16923154, can be taken as the convergence values of the undetermined constants c_0, c_1 and d_0 when q = 0.008 MPa to determine the power series particular solutions of stress and deflection. The results of numerical calculation of stress and deflection at the two ends of the closed interval [4/7, 1], which are calculated by using Equations (24) and (25), are listed in Tables 5 and 6. Figures 16–19 show the variations of $c_i(1-\beta)^i$, $c_i(\alpha-\beta)^i$, $d_i(1-\beta)^i$ and $d_i(\alpha-\beta)^i$ with i, indicating that the power series particular solutions of stress and deflection when q = 0.008 MPa still converge very quickly in comparison with Figures 9–12 (q = 0.0001 MPa).

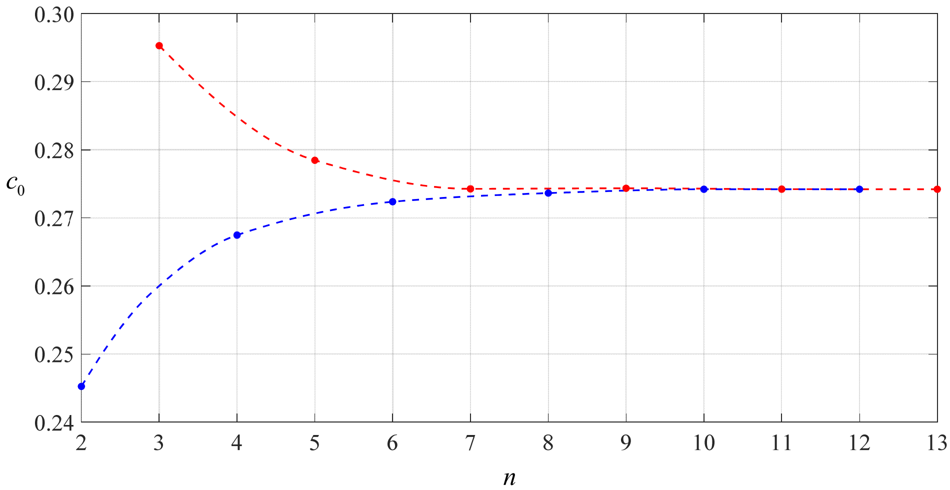

Figure 13. Variation of c_0 with n for q = 0.008 MPa, where the dash-dotted line shows the convergence trend of the data points of even terms (n = 2, 4, 6 . . .) and the dashed line shows that of odd terms (n = 3, 5, 7 . . .).

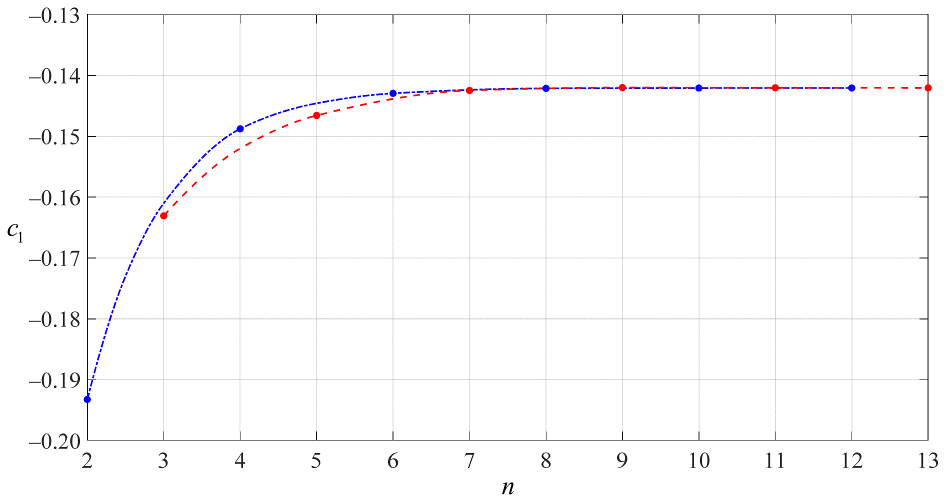

Figure 14. Variation of c_1 with n for q = 0.008 MPa, where the dash-dotted line shows the convergence trend of the data points of even terms (n = 2, 4, 6 . . .) and the dashed line shows that of odd terms (n = 3, 5, 7 . . .).

Combining the above, it can be concluded that the increase in the loads q from 0.0001 MPa to 0.008 MPa mainly affects the determination of the convergence values of the undetermined constants c_0, c_1 and d_0, but has little influence on the convergence of the power series particular solutions of stress and deflection. Therefore, regardless of the magnitude of the applied loads q (corresponding to the different geometry of a deflected annular membrane), the convergence values of the undetermined constants c_0, c_1 and d_0 should be determined in terms of the convergence on the scatter diagrams (such as Figures 3–5 or Figures 13–15). From this point of view, drawing a scatter diagram is a very important work for the power series solution of ordinary differential equations, but in practice, its importance is often ignored.

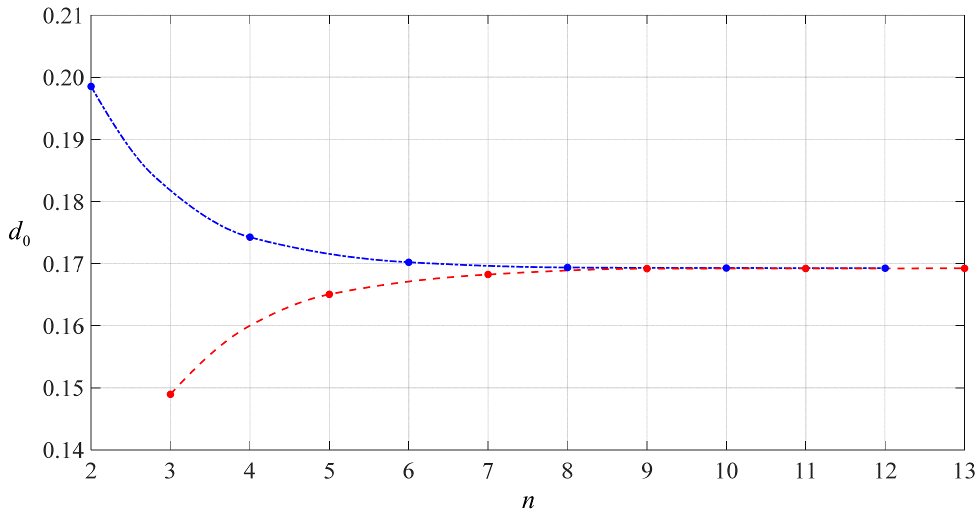

Figure 15. Variation of d_0 with n for q = 0.008 MPa, where the dash-dotted line shows the convergence trend of the data points of even terms (n = 2, 4, 6 ...) and the dashed line shows that of odd terms (n = 3, 5, 7 ...).

Table 5. The numerically calculated values of $c_i(1-\beta)^i$ and $c_i(\alpha-\beta)^i$ when q = 0.008 MPa, α = 4/7 and β = 11/14.

i	$c_i(1-\beta)^i$	$c_i(\alpha-\beta)^i$
0	0.27421591	0.27421591
1	−0.03043674	0.03043674
2	0.00655555	0.00655555
3	−0.00409301	0.00409301
4	$9.57948254 \times 10^{-4}$	$9.57948254 \times 10^{-4}$
5	$-4.72257108 \times 10^{-4}$	$4.72257108 \times 10^{-4}$
6	$8.39765267 \times 10^{-5}$	$8.39765267 \times 10^{-5}$
7	$-5.62440026 \times 10^{-5}$	$5.62440026 \times 10^{-5}$
8	$2.39571485 \times 10^{-6}$	$2.39571485 \times 10^{-6}$
9	$-8.48354140 \times 10^{-6}$	$8.48354140 \times 10^{-6}$
10	$1.71560584 \times 10^{-6}$	$1.71560584 \times 10^{-6}$
11	$-1.92778425 \times 10^{-6}$	$1.92778425 \times 10^{-6}$
12	$8.75934218 \times 10^{-7}$	$8.75934218 \times 10^{-7}$
13	$-6.26245384 \times 10^{-7}$	$6.26245384 \times 10^{-7}$

Table 6. The numerically calculated values of $d_i(1-\beta)^i$ and $d_i(\alpha-\beta)^i$ when q = 0.008 MPa, α = 4/7 and β = 11/14.

i	$d_i(1-\beta)^i$	$d_i(\alpha-\beta)^i$
0	0.16923154	0.16923154
1	−0.12761152	0.12761152
2	−0.03316675	−0.03316675
3	−0.00559019	0.00559019
4	−0.00186868	−0.00186868
5	$-6.72098886 \times 10^{-4}$	$6.72098886 \times 10^{-4}$
6	$-2.62267256 \times 10^{-4}$	$-2.62267256 \times 10^{-4}$
7	$-1.11698057 \times 10^{-4}$	$1.11698057 \times 10^{-4}$
8	$-4.86768405 \times 10^{-5}$	$-4.86768405 \times 10^{-5}$
9	$-2.22870953 \times 10^{-5}$	$2.22870953 \times 10^{-5}$
10	$-1.04435147 \times 10^{-5}$	$-1.04435147 \times 10^{-5}$
11	$-5.03839569 \times 10^{-6}$	$5.03839569 \times 10^{-6}$
12	$-2.48735974 \times 10^{-6}$	$-2.48735974 \times 10^{-6}$
13	$-1.25620215 \times 10^{-6}$	$1.25620215 \times 10^{-6}$

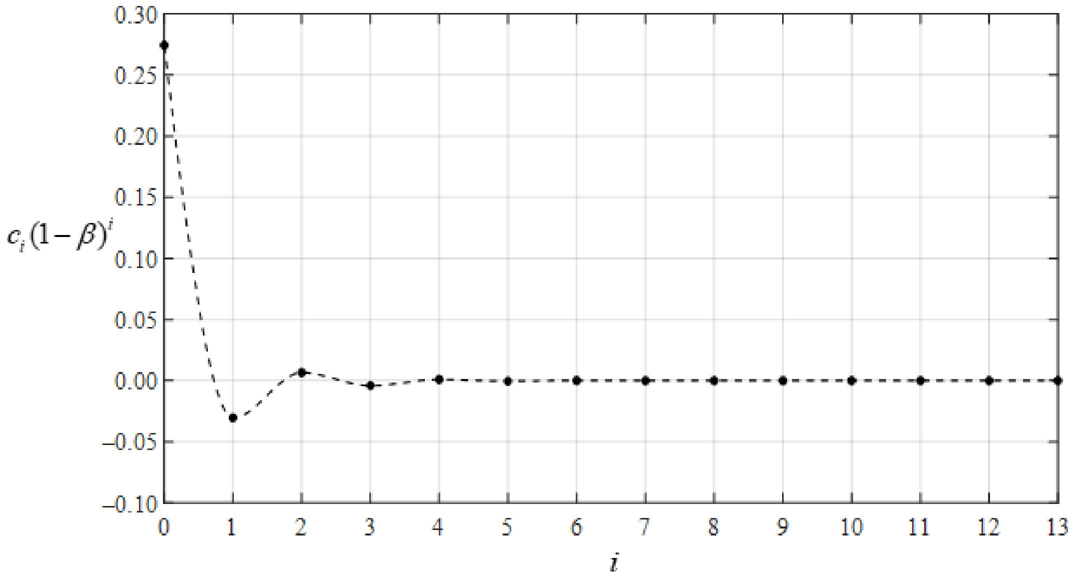

Figure 16. Variation of $c_i(1-\beta)^i$ with i when q = 0.008 MPa and β = 11/14.

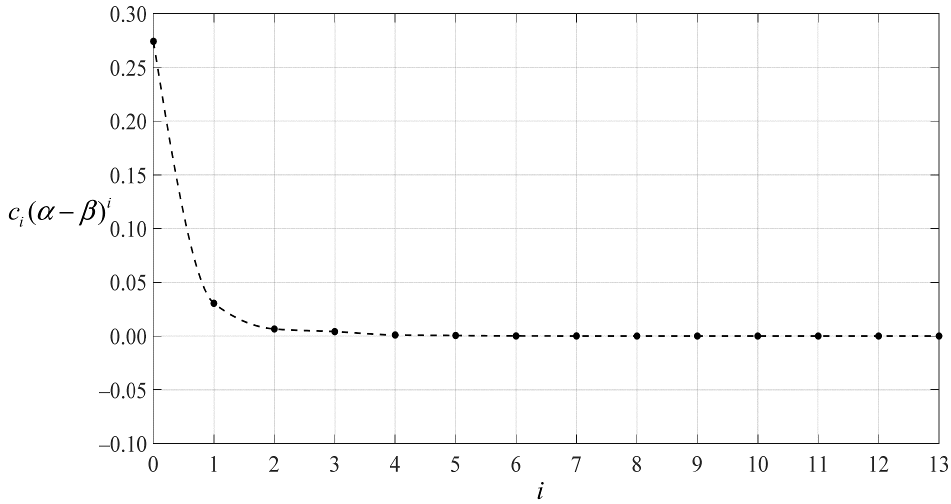

Figure 17. Variation of $c_i(\alpha-\beta)^i$ with i when q = 0.008 MPa, α = 4/7 and β = 11/14.

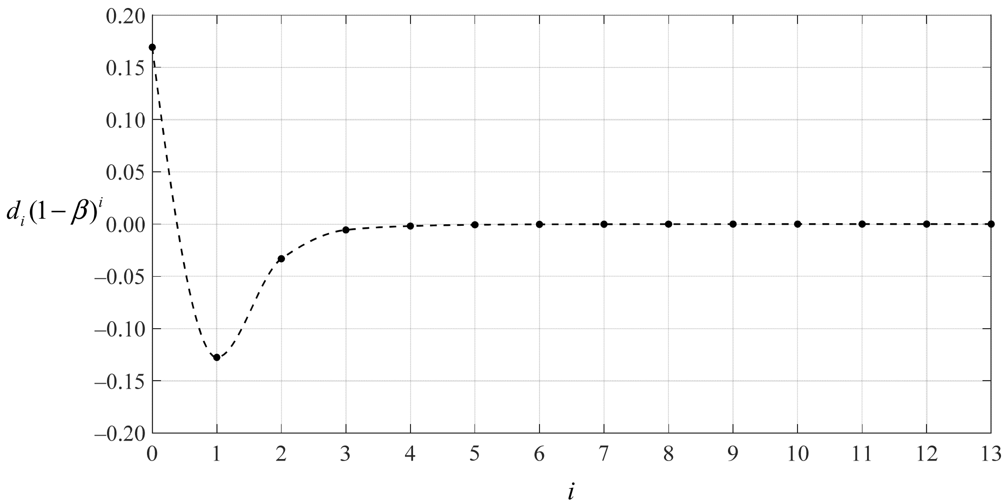

Figure 18. Variation of $d_i(1-\beta)^i$ with i when q = 0.008 MPa and β = 11/14.

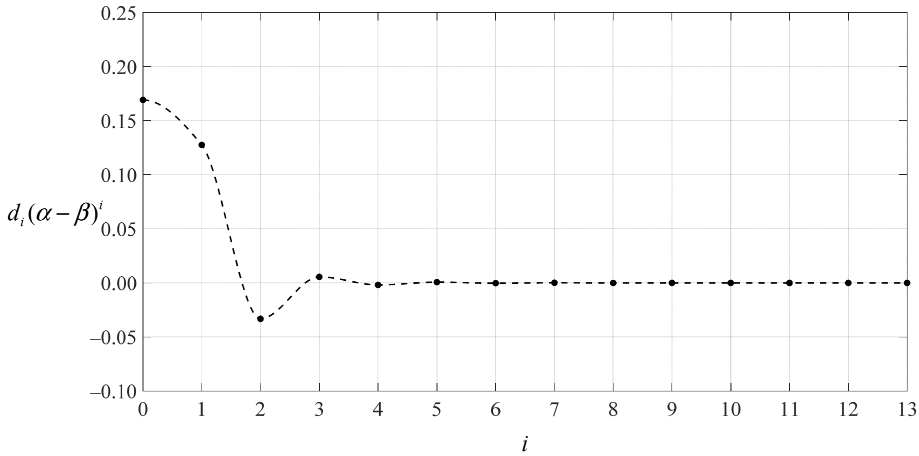

Figure 19. Variation of $d_i(\alpha-\beta)^i$ with i when q = 0.008 MPa, α = 4/7 and β = 11/14.

3.2. Asymptotic Behavior of the Closed-Form Solution

The effectiveness of the closed-form solution obtained in Section 2 may be proved by its asymptotic behavior from an annular membrane to a circular membrane, that is, the closed-form solution of an Alekseev-type annular membrane with outer radius a and inner radius b, which is given in Section 2, should be equivalent to the closed-form solution of a circular membrane with outer radius a, when the inner radius of the annular membrane approaches zero ($b\to 0$). To this end, the closed-form solution of circular membranes presented by Lian et al. in 2020 [23] is specially used here, which is obtained by using the same out-of-plane, in-plane, geometric and physical equations used in this paper. The circular membrane and Alekseev-type annular membrane are subjected to the same action of loads q = 0.0002 MPa and have the same thickness h = 0.2 mm, outer radius a = 70 mm, Poisson's ratio v = 0.47, and Young's modulus of elasticity E = 7.84 MPa, and the inner radius of the Alekseev-type annular membrane takes b = 60 mm, 40 mm, 20 mm and 10 mm, respectively. Their deflection profiles along a diameter are shown in Figure 20, where the solid lines ("Present study") refer to the deflection curves of the Alekseev-type annular membranes, which are calculated by the closed-form solution given in Section 2, and the dash-dotted solid line ("Lian et al., 2020") refers to the deflection curve of the circular membrane, which is calculated by the closed-form solution given by Lian et al. in 2020 [23]. From Figure 20, it can be seen that as the inner radius of the Alekseev-type annular membranes gradually approach zero ($b\to 0$), their deflection curves are gradually closed to the deflection curve of the circular membrane. This indicates that the derivation of the closed-form solution given in Section 2 is, to some extent, correct and reliable.

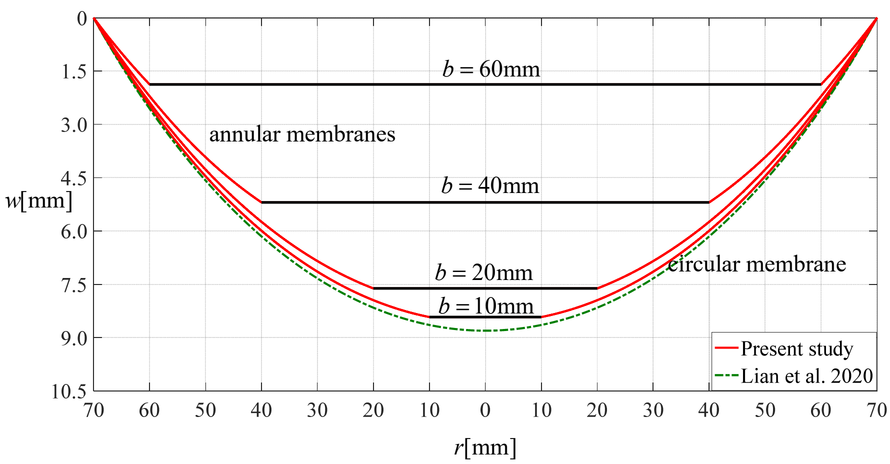

Figure 20. Deflection profiles along a diameter of four Alekseev-type annular membranes and a circular membrane when q = 0.0002 MPa.

3.3. Comparison between Closed-Form Solutions before and after Improvement

To quantitatively analyze the difference between the closed-form solutions before and after improvement (i.e., the closed-form solutions presented by Lian et al. [15] and in this paper), an example is considered of an Alekseev-type annular membrane with thickness h = 0.2 mm, inner radius b = 40 mm, outer radius a = 70 mm, Poisson's ratio v = 0.47 and Young's modulus of elasticity E = 7.84 MPa, which is subjected to the loads q = 0.0002 MPa, 0.008 MPa and 0.035 MPa, respectively. Figures 21 and 22 show the variations of deflection and stress differences with loads q, where the dashed lines ("Lian et al., 2017") are calculated by using the closed-form solution which was presented by Lian et al. in 2017 [15] and the solid lines ("Present study") by using the closed-form solution given in Section 2. It can be seen from Figure 21 that as the uniformly distributed transverse loads q increase from 0.0002 MPa to 0.035 MPa, the differences in deflection also increase, and the differences in maximum deflection are about 5.195 mm − 5.162 mm = 0.033 mm when q = 0.0002 MPa, 18.761 mm − 17.654 mm = 1.107 mm when q = 0.008 MPa, and 32.346 mm − 28.873 mm = 3.473 mm when q = 0.035 MPa. Additionally, it can be seen from Figure 22 that as the uniformly distributed transverse loads q increase from 0.0002 MPa to 0.035 MPa, the differences in stress also increase. The differences in maximum stress are about 0.189518 MPa − 0.187173 MPa = 0.002345 MPa when q = 0.0002 MPa, 2.484320 MPa − 2.189192 MPa = 0.295128 MPa when q = 0.008 MPa, and 8.142192 MPa − 5.856020 MPa = 2.286172 MPa when q = 0.035 MPa, while the differences in minimum stress are about 0.145827 MPa − 0.143930 MPa = 0.001897 MPa when q = 0.0002 MPa, 1.934280 MPa − 1.684316 MPa = 0.250864 MPa when q = 0.008 MPa, and 6.483791 MPa − 4.503084 MPa = 1.980707 MPa when q = 0.035 MPa. Figures 21 and 22 suggest that the closed-form solutions, which are presented by Lian et al. [15] and in this paper, are very close to each other for lightly loaded membranes and diverge gradually as the loads q applied intensifies. Therefore, the closed-form solution presented in this paper should be used preferentially for heavily loaded Alekseev-type annular membranes with larger rotation angles.

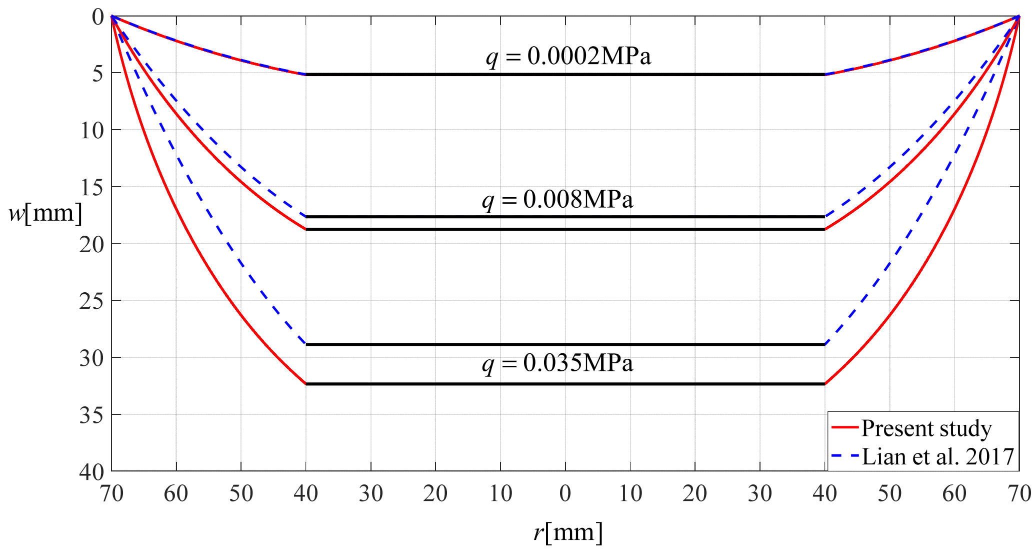

Figure 21. Variations of differences in deflection with loads q.

Now, let us analyze qualitatively the difference between the closed-form solutions before and after improvement from the point of view of the asymptotic behavior of annular membrane solutions gradually approaching circular membrane solutions. We continue with the example in Section 3.2 but increase the loads q from 0.0002 MPa to 0.01 MPa. The deflection profiles along a diameter are shown in Figure 23, where the solid lines ("Present study") refer to the deflection curves of four Alekseev-type annular membranes with outer radius a = 70 mm and inner radius b = 60 mm, 40 mm, 20 mm and 10 mm under q = 0.01 MPa, which are calculated by using the closed-form solution given in Section 2, the dashed lines ("Lian et al., 2017") refer to the deflection curves of four Alekseev-type annular membranes with outer radius a = 70 mm and inner radius b = 60 mm, 40 mm, 20 mm and 10 mm under q = 0.01 MPa, which are calculated by using the closed-form solution presented by Lian et al. in 2017 [15], and the dash-dotted solid line ("Lian et al., 2020") refers to the deflection curve of the circular membrane with outer radius a = 70 mm under q = 0.01 MPa, which is calculated by using the closed-form solution given by Lian et al. in 2020 [23]. It can be seen from Figure 23 that the asymptotic behavior of the "Present study" gradually approaching the "Lian et al., 2020" can still remain constant when q = 0.01 MPa.

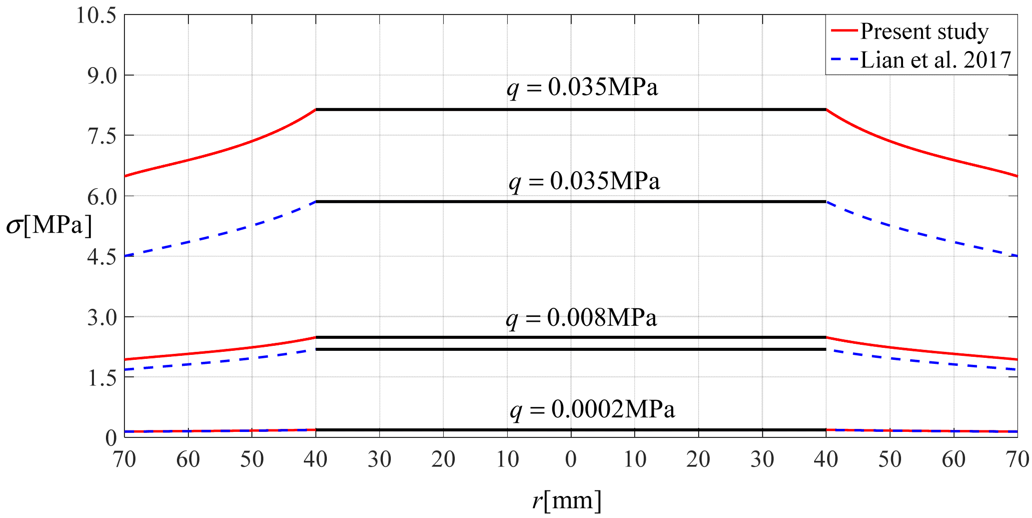

Figure 22. Variations of differences in stress with loads q.

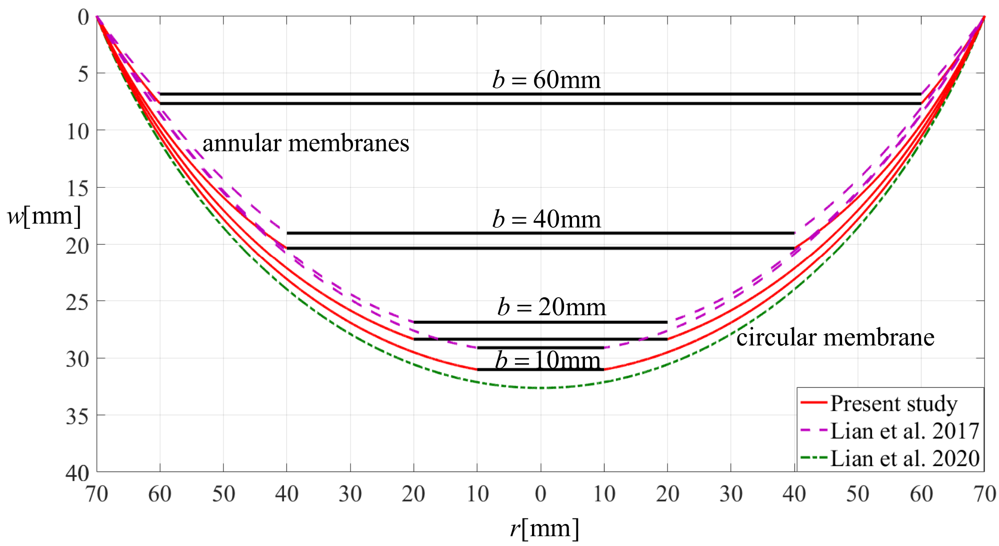

Figure 23. Deflection profiles along a diameter of eight Alekseev-type annular membranes and a circular membrane when q = 0.01 MPa.

However, from Figure 23 it can also be seen that the asymptotic behavior of the "Lian et al., 2017" gradually approaching the "Lian et al., 2020" is, in terms of the effect, inferior to the asymptotic behavior of the "Present study" gradually approaching the "Lian et al., 2020". The gap between the two gradually increases as the inner radius b of the Alekseev-type annular membranes gradually decreases, see Figure 23. So, in theory, when $b \to 0$, if the "Present study" can be close to the "Lian et al., 2020", then the "Lian et al., 2017" will never be close to the "Lian et al., 2020". Therefore, from this point of view, if the "Lian et al., 2020" is used as the benchmark (the closed-form solution of circular membranes presented by Lian et al. in 2020 [23] has certain credibility because it is an improvement on a classic well-established solution, the well-known Hencky solution, see [23] for details), then it can be qualitatively concluded as follows: under the same conditions the closed-form solution presented in this paper has higher computational accuracy than the closed-form solution presented by Lian et al. in 2017 [15].

3.4. Beneficial Effect of Improved Closed-Form Solution on Pressure Measurement

In the pressure measurement systems (using the capacitive pressure sensors proposed by Lian et al. [15]), the maximum deflection w_m of the Alekseev-type annular membranes under pressure q can be determined by capacitance measurement, then the pressure q applied can be determined with the determined maximum deflection w_m and the closed-form solution of the elastic behavior of the Alekseev-type annular membranes under pressure q. Therefore, the beneficial effect of the improved closed-form solution presented in this paper on developing the pressure measurement systems (using the capacitive pressure sensors proposed by Lian et al. [15]) can be directly reflected by the difference of the pressure calculation values, where the closed-form solutions presented in this paper and presented by Lian et al. [15] are used for the pressure calculations under the same maximum deflection w_m.

To this end, the Alekseev-type annular membrane used in Section 3.3 is used again, i.e., thickness h = 0.2 mm, inner radius b = 40 mm, outer radius a = 70 mm, Poisson's ratio v = 0.47 and Young's modulus of elasticity E = 7.84 MPa. Let this Alekseev-type annular membrane first subjected to the loads q = 0.0002 MPa, 0.008 MPa and 0.035 MPa, respectively, where the maximum deflections produced are w_m = 5.195 mm for q = 0.0002 MPa, w_m = 18.761 mm for q = 0.008 MPa, and w_m = 32.346 mm for q = 0.035 MPa, which are calculated by using the closed-form solution presented in this paper. Then, use the closed-form solution presented by Lian et al. [15] to calculate the pressure q required when this Alekseev-type annular membrane produces the same maximum deflections w_m, i.e., w_m = 5.195 mm, 18.761 mm and 32.346 mm, respectively. These calculations result in that w_m = 5.195 mm requires about q = 0.000204 MPa, w_m = 18.761 mm requires about q = 0.0096 MPa, and w_m = 32.346 mm requires about q = 0.0492 MPa, respectively. For the sake of intuition and clarity, the calculation results are listed in Table 7 and shown in Figure 24, where the "Present study" refers to the results calculated by using the closed-form solution given in Section 2 and the "Lian et al., 2017" refers to the results calculated by using the closed-form solution which was given by Lian et al. in 2017 [15]. It can be seen from Table 7 that as the maximum deflection w_m increases from 5.195 mm to 32.346 mm (the ratio of maximum deflection to diameter of the annular membrane is about 0.037 to 0.231), the relative errors of "Lian et al., 2017" with respect to "Present study" increases from 2% to 40.57%. This is because the increase in the maximum deflection w_m makes the rotation angle of the annular membrane bigger and bigger, so that the small rotation angle assumption used for establishing the out-of-plane equilibrium equation and geometric equation in [15], i.e., Equations (4) and (6) in [15], is less and less valid due to the bigger and bigger rotation angle. So, if the closed-form solution which was presented by Lian et al. in 2017 [15] is used to predict the pressure q required for a certain maximum deflection w_m determined by capacitance measurement, then the resulting error will increase with the increase in the maximum deflection w_m. Therefore, the closed-form solution presented in this paper should be used preferentially for the pressure measurement systems using the capacitive pressure sensors proposed in [15].

Table 7. Required pressures q and their relative errors under the same maximum deflections w_m.

Maximum Deflections w_m [mm]	Required Pressures q [MPa]		Relative Errors
	Lian et al., 2017	Present Study	
5.195	0.000204	0.0002	2%
18.761	0.0096	0.008	20%
32.346	0.0492	0.035	40.57%

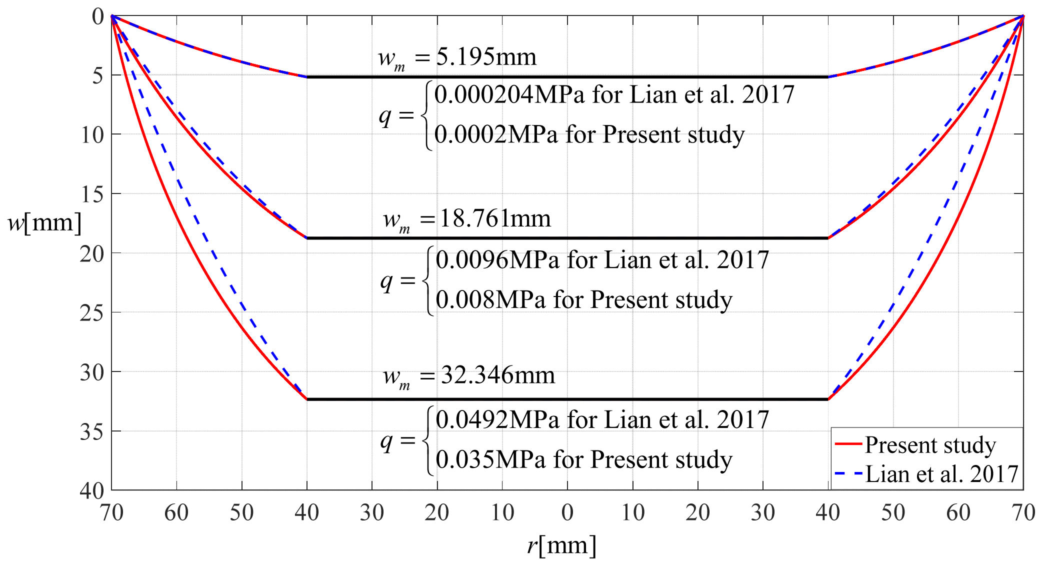

Figure 24. Variations of differences in pressure q with maximum deflection $w_{\rm m}$.

4. Concluding Remarks

In this paper, the axisymmetric deformation problem of an Alekseev-type annular membrane structure under uniformly distributed transverse loads, which was originally proposed in our previous work [15], is investigated again. The main improvement on our previous work is that the assumption of small rotation angle of membrane, which was used in the establishment of the previous out-of-plane equilibrium equation and geometric equations, is given up, resulting in a new and more refined closed-form solution. The following main conclusions can be drawn from this study.

Since the size of the rotation angle of the annular membrane corresponds to the size of the maximum deflection of the annular membrane, the assumption of small rotation angle of membrane will become less and less valid with the increase in the maximum deflection of the annular membrane, making the previous closed-form solution obtained by using the assumption of small rotation angle of membrane become less and less accurate. Therefore, the closed-form solution, which is presented in this paper, should be preferred for the design of the capacitive pressure sensors proposed in [15], in order to reduce pressure measurement error. When the ratio of maximum deflection to diameter of the annular membrane is in the range of 0.037 to 0.231, the pressure measurement error is reduced by about 2% to 40%, indicating that the improvement on our previous work has produced a significant beneficial effect.

The work presented here can be further combined with the design of the capacitive pressure sensors proposed in [15].

Author Contributions: Conceptualization, J.-Y.S.; methodology, B.L., Q.Z. and J.-Y.S.; validation, X.L. and X.-T.H.; writing—original draft preparation, B.L. and Q.Z.; writing—review and editing, X.L. and X.-T.H.; visualization, B.L. and Q.Z.; funding acquisition, J.-Y.S. All authors have read and agreed to the published version of the manuscript.

Funding: This research was funded by the National Natural Science Foundation of China (Grant No. 11772072).

Institutional Review Board Statement: Not applicable.

Informed Consent Statement: Not applicable.

Data Availability Statement: Not applicable.

Conflicts of Interest: The authors declare no conflict of interest.

Nomenclature

a	Outer radius of the annular membrane
b	Inner radius of the annular membrane
h	Thickness of the annular membrane
v	Poisson's ratio
E	Young's modulus of elasticity
q	Uniformly distributed transverse loads
r	Radial coordinate
φ	Angle coordinate
w	Transverse coordinate and deflection
o	Coordinate origin
π	Pi (ratio of circumference to diameter)
σ_r	Radial stress
σ_t	Circumferential stress
θ	Rotation angle of the deflected membrane
e_r	Radial strain
e_t	Circumferential strain
u	Radial displacement
Q	Dimensionless q (aq/hE)
W	Dimensionless w (w/a)
S_r	Dimensionless σ_r (σ_r/E)
S_t	Dimensionless σ_t (σ_t/E)
α	Ratio v of b to a (b/a)
x	Dimensionless r (r/a)
β	Introduced parameter β=(1+α)/2
c_i	Coefficients of the power series for S_r
d_i	Coefficients of the power series for W

Appendix A

$$d_1 = -\frac{\beta Q}{\sqrt{-Q^2\beta^2+4c_0^2}},$$

$$c_2 = \frac{1}{2\beta^2}\left(\sqrt{\beta^2\nu^2{c_1}^2 + 2\beta\nu^2c_0c_1 - 2\beta\nu c_0c_1 + \nu^2{c_0}^2 - 2\beta\nu c_1 - 2\nu{c_0}^2 - 2\nu c_0 + {c_0}^2 - {d_1}^2 + 2c_0 + 1}\right.$$
$$\left.+\beta\nu c_1 - 3\beta c_1 + \nu c_0 - c_0 - 1\right),$$

$$d_2 = -\frac{Q^2\beta{d_1}^2 - 4c_0c_1{d_1}^2 + Q^2\beta}{2d_1(Q^2\beta^2 - 4{c_0}^2)},$$

$$c_3 = \frac{1}{6\beta^2(2\beta^2c_2 - \beta\nu c_1 + 3\beta c_1 - \nu c_0 + c_0 + 1)}(4\beta^3\nu{c_2}^2 - 20\beta^3{c_2}^2 + 20\beta^2\nu c_1c_2 - 38\beta^2c_1c_2$$
$$+10\beta\nu c_0c_2 + 9\beta\nu{c_1}^2 - 10\beta c_0c_2 - 12\beta{c_1}^2 + 3\nu c_0c_1 - 10\beta c_2 - 3c_0c_1 - 2d_1d_2 - 3c_1),$$

$$d_3 = -\frac{1}{6d_1(Q^2\beta^2 - 4{c_0}^2)}(4Q^2\beta^2{d_2}^2 + 8Q^2\beta d_1d_2 + Q^2{d_1}^2 - 16{c_0}^2{d_2}^2$$
$$-32c_0c_1d_1d_2 - 8c_0c_2{d_1}^2 - 4{c_1}^2{d_1}^2 + Q^2),$$

$$c_4 = -\frac{1}{24\beta^2(2\beta^2c_2 - \beta\nu c_1 + 3\beta c_1 - \nu c_0 + c_0 + 1)}(36\beta^4{c_3}^2 - 36\beta^3\nu c_2c_3 + 204\beta^3c_2c_3$$
$$-84\beta^2\nu c_1c_3 - 52\beta^2\nu{c_2}^2 + 174\beta^2c_1c_3 + 136\beta^2{c_2}^2 - 42\beta\nu c_0c_3 - 86\beta\nu c_1c_2 + 42\beta c_0c_3$$
$$+134\beta c_1c_2 - 16\nu c_0c_2 - 12\nu{c_1}^2 + 42\beta c_3 + 16c_0c_2 + 15{c_1}^2 + 6d_1d_3 + 4{d_2}^2 + 16c_2),$$

$$d_4 = -\frac{1}{2d_1(Q^2\beta^2 - 4{c_0}^2)}(3Q^2\beta^2d_2d_3 + 3Q^2\beta d_1d_3 + 2Q^2\beta{d_2}^2 + Q^2d_1d_2 - 12{c_0}^2d_2d_3$$
$$-12c_0c_1d_1d_3 - 8c_0c_1{d_2}^2 - 8c_0c_2d_1d_2 - 2c_0c_3{d_1}^2 - 4{c_1}^2d_1d_2 - 2c_1c_2{d_1}^2),$$

$$c_5 = -\frac{1}{20\beta^2(2\beta^2c_2-\beta\nu c_1+3\beta c_1-\nu c_0+c_0+1)}(72\beta^4c_3c_4 - 32\beta^3\nu c_2c_4 - 18\beta^3\nu c_3{}^2 + 192\beta^3c_2c_4 + 126\beta^3c_3{}^2 - 72\beta^2\nu c_1c_4 - 98\beta^2\nu c_2c_3 + 156\beta^2c_1c_4 + 296\beta^2c_2c_3 - 36\beta\nu c_0c_4 - 78\beta\nu c_1c_3 - 46\beta\nu c_2{}^2 + 36\beta c_0c_4 + 132\beta c_1c_3 + 90\beta c_2{}^2 - 15\nu c_0c_3 - 25\nu c_1c_2 + 36\beta c_4 + 15c_0c_3 + 35c_1c_2 + 4d_1d_4 + 6d_2d_3 + 15c_3),$$

$$d_5 = -\frac{1}{10d_1(Q^2\beta^2-4c_0{}^2)}(16Q^2\beta^2d_2d_4 + 9Q^2\beta^2d_3{}^2 + 16Q^2\beta d_1d_4 + 24Q^2\beta d_2d_3 + 6Q^2d_1d_3 + 4Q^2d_2{}^2 - 64c_0{}^2d_2d_4 - 36c_0{}^2d_3{}^2 - 64c_0c_1d_1d_4 - 96c_0c_1d_2d_3 - 48c_0c_2d_1d_3 - 32c_0c_2d_2{}^2 - 32c_0c_3d_1d_2 - 8c_0c_4d_1{}^2 - 24c_1{}^2d_1d_3 - 16c_1{}^2d_2{}^2 - 32c_1c_2d_1d_2 - 8c_1c_3d_1{}^2 - 4c_2{}^2d_1{}^2),$$

$$c_6 = -\frac{1}{60\beta^2(2\beta^2c_2-\beta\nu c_1+3\beta c_1-\nu c_0+c_0+1)}(240\beta^4c_3c_5 + 144\beta^4c_4{}^2 - 100\beta^3\nu c_2c_5 - 120\beta^3\nu c_3c_4 + 620\beta^3c_2c_5 + 936\beta^3c_3c_4 - 220\beta^2\nu c_1c_5 - 316\beta^2\nu c_2c_4 - 174\beta^2\nu c_3{}^2 + 490\beta^2c_1c_5 + 1036\beta^2c_2c_4 + 633\beta^2c_3{}^2 - 110\beta\nu c_0c_5 - 246\beta\nu c_1c_4 - 314\beta\nu c_2c_3 + 110\beta c_0c_5 + 438\beta c_1c_4 + 698\beta c_2c_3 - 48\nu c_0c_4 - 84\nu c_1c_3 - 48\nu c_2{}^2 + 110\beta c_5 + 48c_0c_4 + 126c_1c_3 + 80c_2{}^2 + 10d_1d_5 + 16d_2d_4 + 9d_3{}^2 + 48c_4),$$

$$d_6 = -\frac{1}{6d_1(Q^2\beta^2-4c_0{}^2)}(10Q^2\beta^2d_2d_5 + 12Q^2\beta^2d_3d_4 + 10Q^2\beta d_1d_5 + 16Q^2\beta d_2d_4 + 9Q^2\beta d_3{}^2 + 4Q^2d_1d_4 + 6Q^2d_2d_3 - 40c_0{}^2d_2d_5 - 48c_0{}^2d_3d_4 - 40c_0c_1d_1d_5 - 64c_0c_1d_2d_4 - 36c_0c_1d_3{}^2 - 32c_0c_2d_1d_4 - 48c_0c_2d_2d_3 - 24c_0c_3d_1d_3 - 16c_0c_3d_2{}^2 - 16c_0c_4d_1d_2 - 4c_0c_5d_1{}^2 - 16c_1{}^2d_1d_4 - 24c_1{}^2d_2d_3 - 24c_1c_2d_1d_3 - 16c_1c_2d_2{}^2 - 16c_1c_3d_1d_2 - 4c_1c_4d_1{}^2 - 8c_2{}^2d_1d_2 - 4c_2c_3d_1{}^2),$$

$$c_7 = -\frac{1}{42\beta^2(2\beta^2c_2-\beta\nu c_1+3\beta c_1-\nu c_0+c_0+1)}(180\beta^4c_3c_6 + 240\beta^4c_4c_5 - 72\beta^3\nu c_2c_6 - 90\beta^3\nu c_3c_5 - 48\beta^3\nu c_4{}^2 + 456\beta^3c_2c_6 + 750\beta^3c_3c_5 + 432\beta^3c_4{}^2 - 156\beta^2\nu c_1c_6 - 232\beta^2\nu c_2c_5 - 270\beta^2\nu c_3c_4 + 354\beta^2c_1c_6 + 802\beta^2c_2c_5 + 1098\beta^2c_3c_4 - 78\beta\nu c_0c_6 - 178\beta\nu c_1c_5 - 238\beta\nu c_2c_4 - 129\beta\nu c_3{}^2 + 78\beta c_0c_6 + 328\beta c_1c_5 + 574\beta c_2c_4 + 336\beta c_3{}^2 - 35\nu c_0c_5 - 63\nu c_1c_4 - 77\nu c_2c_3 + 78\beta c_6 + 35c_0c_5 + 99c_1c_4 + 143c_2c_3 + 6d_1d_6 + 10d_2d_5 + 12d_3d_4 + 35c_5),$$

$$d_7 = -\frac{1}{14d_1(Q^2\beta^2-4c_0{}^2)}(24Q^2\beta^2d_2d_6 + 30Q^2\beta^2d_3d_5 + 16Q^2\beta^2d_4{}^2 + 24Q^2\beta d_1d_6 + 40Q^2\beta d_2d_5 + 48Q^2\beta d_3d_4 + 10Q^2d_1d_5 + 16Q^2d_2d_4 + 9Q^2d_3{}^2 - 96c_0{}^2d_2d_6 - 120c_0{}^2d_3d_5 - 64c_0{}^2d_4{}^2 - 96c_0c_1d_1d_6 - 160c_0c_1d_2d_5 - 192c_0c_1d_3d_4 - 80c_0c_2d_1d_5 - 128c_0c_2d_2d_4 - 72c_0c_2d_3{}^2 - 64c_0c_3d_1d_4 - 96c_0c_3d_2d_3 - 48c_0c_4d_1d_3 - 32c_0c_4d_2{}^2 - 32c_0c_5d_1d_2 - 8c_0c_6d_1{}^2 - 40c_1{}^2d_1d_5 - 64c_1{}^2d_2d_4 - 36c_1{}^2d_3{}^2 - 64c_1c_2d_1d_4 - 96c_1c_2d_2d_3 - 48c_1c_3d_1d_3 - 32c_1c_3d_2{}^2 - 32c_1c_4d_1d_2 - 8c_1c_5d_1{}^2 - 24c_2{}^2d_1d_3 - 16c_2{}^2d_2{}^2 - 32c_2c_3d_1d_2 - 8c_2c_4d_1{}^2 - 4c_3{}^2d_1{}^2),$$

$$c_8 = -\frac{1}{112\beta^2(2\beta^2c_2-\beta\nu c_1+3\beta c_1-\nu c_0+c_0+1)}(504\beta^4c_3c_7 + 720\beta^4c_4c_6 + 400\beta^4c_5{}^2 - 196\beta^3\nu c_2c_7 - 252\beta^3\nu c_3c_6 - 280\beta^3\nu c_4c_5 + 1260\beta^3c_2c_7 + 2196\beta^3c_3c_6 + 2760\beta^3c_4c_5 - 420\beta^2\nu c_1c_7 - 640\beta^2\nu c_2c_6 - 772\beta^2\nu c_3c_5 - 408\beta^2\nu c_4{}^2 + 966\beta^2c_1c_7 + 2296\beta^2c_2c_6 + 3382\beta^2c_3c_5 + 1896\beta^2c_4{}^2 - 210\beta\nu c_0c_7 - 486\beta\nu c_1c_6 - 670\beta\nu c_2c_5 - 762\beta\nu c_3c_4 + 210\beta c_0c_7 + 918\beta c_1c_6 + 1710\beta c_2c_5 + 2202\beta c_3c_4 - 96\nu c_0c_6 - 176\nu c_1c_5 - 224\nu c_2c_4 - 120\nu c_3{}^2 + 210\beta c_7 + 96c_0c_6 + 286c_1c_5 + 448c_2c_4 + 255c_3{}^2 + 14d_1d_7 + 24d_2d_6 + 30d_3d_5 + 16d_4{}^2 + 96c_6),$$

$$
\begin{aligned}
d_8 = -&\tfrac{1}{4d_1(Q^2\beta^2-4c_0{}^2)}(7Q^2\beta^2d_2d_7+9Q^2\beta^2d_3d_6+10Q^2\beta^2d_4d_5+7Q^2\beta d_1d_7\\
&+12Q^2\beta d_2d_6+15Q^2\beta d_3d_5+8Q^2\beta d_4{}^2+3Q^2d_1d_6+5Q^2d_2d_5+6Q^2d_3d_4-28c_0{}^2d_2d_7\\
&-36c_0{}^2d_3d_6-40c_0{}^2d_4d_5-28c_0c_1d_1d_7-48c_0c_1d_2d_6-60c_0c_1d_3d_5-32c_0c_1d_4{}^2\\
&-24c_0c_2d_1d_6-40c_0c_2d_2d_5-48c_0c_2d_3d_4-20c_0c_3d_1d_5-32c_0c_3d_2d_4-18c_0c_3d_3{}^2\\
&-16c_0c_4d_1d_4-24c_0c_4d_2d_3-12c_0c_5d_1d_3-8c_0c_5d_2{}^2-8c_0c_6d_1d_2-2c_0c_7d_1{}^2-12c_1{}^2d_1d_6\\
&-20c_1{}^2d_2d_5-24c_1{}^2d_3d_4-20c_1c_2d_1d_5-32c_1c_2d_2d_4-18c_1c_2d_3{}^2-16c_1c_3d_1d_4\\
&-24c_1c_3d_2d_3-12c_1c_4d_1d_3-8c_1c_4d_2{}^2-8c_1c_5d_1d_2-2c_1c_6d_1{}^2-8c_2{}^2d_1d_4-12c_2{}^2d_2d_3\\
&-12c_2c_3d_1d_3-8c_2c_3d_2{}^2-8c_2c_4d_1d_2-2c_2c_5d_1{}^2-4c_3{}^2d_1d_2-2c_3c_4d_1{}^2)
\end{aligned},
$$

$$
\begin{aligned}
c_9 = -&\tfrac{1}{72\beta^2(2\beta^2c_2-\beta\nu c_1+3\beta c_1-\nu c_0+c_0+1)}(336\beta^4c_3c_8+504\beta^4c_4c_7+600\beta^4c_5c_6\\
&-128\beta^3\nu c_2c_8-168\beta^3\nu c_3c_7-192\beta^3\nu c_4c_6-100\beta^3\nu c_5{}^2+832\beta^3c_2c_8+1512\beta^3c_3c_7\\
&+2016\beta^3c_4c_6+1100\beta^3c_5{}^2-272\beta^2\nu c_1c_8-422\beta^2\nu c_2c_7-522\beta^2\nu c_3c_6-572\beta^2\nu c_4c_5\\
&+632\beta^2c_1c_8+1556\beta^2c_2c_7+2412\beta^2c_3c_6+2912\beta^2c_4c_5-136\beta\nu c_0c_8-318\beta\nu c_1c_7\\
&-448\beta\nu c_2c_6-526\beta\nu c_3c_5-276\beta\nu c_4{}^2+136\beta c_0c_8+612\beta c_1c_7+1192\beta c_2c_6\\
&+1636\beta c_3c_5+900\beta c_4{}^2-63\nu c_0c_7-117\nu c_1c_6-153\nu c_2c_5-171\nu c_3c_4+136\beta c_8\\
&+63c_0c_7+195c_1c_6+323c_2c_5+399c_3c_4+8d_1d_8+14d_2d_7+18d_3d_6+20d_4d_5+63c_7)
\end{aligned},
$$

$$
\begin{aligned}
d_9 = -&\tfrac{1}{18d_1(Q^2\beta^2-4c_0{}^2)}(32Q^2\beta^2d_2d_8+42Q^2\beta^2d_3d_7+48Q^2\beta^2d_4d_6+25Q^2\beta^2d_5{}^2\\
&+32Q^2\beta d_1d_8+56Q^2\beta d_2d_7+72Q^2\beta d_3d_6+80Q^2\beta d_4d_5+14Q^2d_1d_7+24Q^2d_2d_6\\
&+30Q^2d_3d_5+16Q^2d_4{}^2-128c_0{}^2d_2d_8-168c_0{}^2d_3d_7-192c_0{}^2d_4d_6-100c_0{}^2d_5{}^2\\
&-128c_0c_1d_1d_8-224c_0c_1d_2d_7-288c_0c_1d_3d_6-320c_0c_1d_4d_5-112c_0c_2d_1d_7-192c_0c_2d_2d_6\\
&-240c_0c_2d_3d_5-128c_0c_2d_4{}^2-96c_0c_3d_1d_6-160c_0c_3d_2d_5-192c_0c_3d_3d_4-80c_0c_4d_1d_5\\
&-128c_0c_4d_2d_4-72c_0c_4d_3{}^2-64c_0c_5d_1d_4-96c_0c_5d_2d_3-48c_0c_6d_1d_3-32c_0c_6d_2{}^2\\
&-32c_0c_7d_1d_2-8c_0c_8d_1{}^2-56c_1{}^2d_1d_7-96c_1{}^2d_2d_6-120c_1{}^2d_3d_5-64c_1{}^2d_4{}^2-96c_1c_2d_1d_6\\
&-160c_1c_2d_2d_5-192c_1c_2d_3d_4-80c_1c_3d_1d_5-128c_1c_3d_2d_4-72c_1c_3d_3{}^2-64c_1c_4d_1d_4\\
&-96c_1c_4d_2d_3-48c_1c_5d_1d_3-32c_1c_5d_2{}^2-32c_1c_6d_1d_2-8c_1c_7d_1{}^2-40c_2{}^2d_1d_5-64c_2{}^2d_2d_4\\
&-36c_2{}^2d_3{}^2-64c_2c_3d_1d_4-96c_2c_3d_2d_3-48c_2c_4d_1d_3-32c_2c_4d_2{}^2-32c_2c_5d_1d_2-8c_2c_6d_1{}^2\\
&-24c_3{}^2d_1d_3-16c_3{}^2d_2{}^2-32c_3c_4d_1d_2-8c_3c_5d_1{}^2-4c_4{}^2d_1{}^2)
\end{aligned},
$$

$$
\begin{aligned}
c_{10} = -&\tfrac{1}{180\beta^2(2\beta^2c_2-\beta\nu c_1+3\beta c_1-\nu c_0+c_0+1)}(864\beta^4c_3c_9+1344\beta^4c_4c_8\\
&+1680\beta^4c_5c_7+900\beta^4c_6{}^2-324\beta^3\nu c_2c_9-432\beta^3\nu c_3c_8+2124\beta^3c_2c_9\\
&+3984\beta^3c_3c_8+5544\beta^3c_4c_7+6420\beta^3c_5c_6-684\beta^2\nu c_1c_9-1076\beta^2\nu c_2c_8\\
&-1356\beta^2\nu c_3c_7-1524\beta^2\nu c_4c_6-790\beta^2\nu c_5{}^2+4465\beta^2c_5{}^2+3170\beta c_2c_7+4554\beta c_3c_6\\
&-160\nu c_0c_8-300\nu c_1c_7-400\nu c_2c_6-460\nu c_3c_5+18d_1d_9+32d_2d_8+42d_3d_7+48d_4d_6\\
&+1602\beta^2c_1c_9+4052\beta^2c_2c_8+6522\beta^2c_3c_7+8292\beta^2c_4c_6-342\beta\nu c_0c_9-806\beta\nu c_1c_8\\
&-1154\beta\nu c_2c_7-1386\beta\nu c_3c_6-1502\beta\nu c_4c_5+342\beta c_0c_9+1574\beta c_1c_8+5342\beta c_4c_5\\
&+342\beta c_9+1150c_3c_5+160c_8-504\beta^3\nu c_4c_7-540\beta^3\nu c_5c_6-240\nu c_4{}^2+160c_0c_8\\
&+510c_1c_7+880c_2c_6+624c_4{}^2+25d_5{}^2)
\end{aligned},
$$

$$d_{10} = -\frac{1}{10d_1(Q^2\beta^2-4c_0{}^2)}\begin{pmatrix} 18Q^2\beta^2 d_2 d_9 + 24Q^2\beta^2 d_3 d_8 + 28Q^2\beta^2 d_4 d_7 + 30Q^2\beta^2 d_5 d_6 \\ +18Q^2\beta d_1 d_9 + 32Q^2\beta d_2 d_8 + 42Q^2\beta d_3 d_7 + 48Q^2\beta d_4 d_6 + 25Q^2\beta d_5{}^2 + 8Q^2 d_1 d_8 \\ +14Q^2 d_2 d_7 + 18Q^2 d_3 d_6 + 20Q^2 d_4 d_5 - 72c_0{}^2 d_2 d_9 - 96c_0{}^2 d_3 d_8 - 112c_0{}^2 d_4 d_7 \\ -120c_0{}^2 d_5 d_6 - 72c_0 c_1 d_1 d_9 - 128c_0 c_1 d_2 d_8 - 168c_0 c_1 d_3 d_7 - 192c_0 c_1 d_4 d_6 - 100c_0 c_1 d_5{}^2 \\ -64c_0 c_2 d_1 d_8 - 112c_0 c_2 d_2 d_7 - 144c_0 c_2 d_3 d_6 - 160c_0 c_2 d_4 d_5 - 56c_0 c_3 d_1 d_7 - 96c_0 c_3 d_2 d_6 \\ -120c_0 c_3 d_3 d_5 - 64c_0 c_3 d_4{}^2 - 48c_0 c_4 d_1 d_6 - 80c_0 c_4 d_2 d_5 - 96c_0 c_4 d_3 d_4 - 40c_0 c_5 d_1 d_5 \\ -64c_0 c_5 d_2 d_4 - 36c_0 c_5 d_3{}^2 - 32c_0 c_6 d_1 d_4 - 48c_0 c_6 d_2 d_3 - 24c_0 c_7 d_1 d_3 - 16c_0 c_7 d_2{}^2 \\ -16c_0 c_8 d_1 d_2 - 4c_0 c_9 d_1{}^2 - 32c_1{}^2 d_1 d_8 - 56c_1{}^2 d_2 d_7 - 72c_1{}^2 d_3 d_6 - 80c_1{}^2 d_4 d_5 - 56c_1 c_2 d_1 d_7 \\ -96c_1 c_2 d_2 d_6 - 120c_1 c_2 d_3 d_5 - 64c_1 c_2 d_4{}^2 - 48c_1 c_3 d_1 d_6 - 80c_1 c_3 d_2 d_5 - 96c_1 c_3 d_3 d_4 \\ -40c_1 c_4 d_1 d_5 - 64c_1 c_4 d_2 d_4 - 36c_1 c_4 d_3{}^2 - 32c_1 c_5 d_1 d_4 - 48c_1 c_5 d_2 d_3 - 24c_1 c_6 d_1 d_3 \\ -16c_1 c_6 d_2{}^2 - 16c_1 c_7 d_1 d_2 - 4c_1 c_8 d_1{}^2 - 24c_2{}^2 d_1 d_6 - 40c_2{}^2 d_2 d_5 - 48c_2{}^2 d_3 d_4 - 40c_2 c_3 d_1 d_5 \\ -64c_2 c_3 d_2 d_4 - 36c_2 c_3 d_3{}^2 - 32c_2 c_4 d_1 d_4 - 48c_2 c_4 d_2 d_3 - 24c_2 c_5 d_1 d_3 - 16c_2 c_5 d_2{}^2 \\ -16c_2 c_6 d_1 d_2 - 4c_2 c_7 d_1{}^2 - 16c_3{}^2 d_1 d_4 - 24c_3{}^2 d_2 d_3 - 24c_3 c_4 d_1 d_3 - 16c_3 c_4 d_2{}^2 - 16c_3 c_5 d_1 d_2 \\ -4c_3 c_6 d_1{}^2 - 8c_4{}^2 d_1 d_2 - 4c_4 c_5 d_1{}^2 \end{pmatrix},$$

$$c_{11} = -\frac{1}{110\beta^2(2\beta^2 c_2 - \beta\nu c_1 + 3\beta c_1 - \nu c_0 + c_0 + 1)}\begin{pmatrix} -200\beta^3\nu c_2 c_{10} - 270\beta^3\nu c_3 c_9 \\ -320\beta^3\nu c_4 c_8 - 350\beta^3\nu c_5 c_7 - 420\beta^2\nu c_1 c_{10} - 854\beta^2\nu c_3 c_8 - 978\beta^2\nu c_4 c_7 \\ -1040\beta^2\nu c_5 c_6 + 5598\beta^2 c_4 c_7 - 210\beta\nu c_0 c_{10} - 498\beta\nu c_1 c_9 - 722\beta\nu c_2 c_8 \\ -882\beta\nu c_3 c_7 - 978\beta\nu c_4 c_6 - 505\beta\nu c_5{}^2 + 2034\beta c_2 c_8 + 3024\beta c_3 c_7 + 3714\beta c_4 c_6 \\ +99c_9 + 540\beta^4 c_3 c_{10} + 864\beta^4 c_4 c_9 + 1260\beta^4 c_6 c_7 - 668\beta^2\nu c_2 c_9 + 6350\beta^2 c_5 c_6 \\ +210\beta c_0 c_{10} - 99\nu c_0 c_9 - 187\nu c_1 c_8 - 253\nu c_2 c_7 - 297\nu c_3 c_6 - 319\nu c_4 c_5 - 180\beta^3\nu c_6{}^2 \\ +1120\beta^4 c_5 c_8 + 4238\beta^2 c_3 c_8 + 2558\beta^2 c_2 c_9 + 10d_1 d_{10} + 18d_2 d_9 + 24d_3 d_8 + 28d_4 d_7 \\ +30d_5 d_6 + 2340\beta^3 c_6{}^2 + 990\beta^2 c_1 c_{10} + 1980\beta c_5{}^2 + 99c_0 c_9 + 323c_1 c_8 + 575c_2 c_7 \\ +783c_3 c_6 + 899c_4 c_5 + 210\beta c_{10} + 1320\beta^3 c_2 c_{10} + 2538\beta^3 c_3 c_9 + 3648\beta^3 c_4 c_8 \\ +984\beta c_1 c_9 + 4410\beta^3 c_5 c_7 \end{pmatrix},$$

$$d_{11} = -\frac{1}{22d_1(Q^2\beta^2-4c_0{}^2)}\begin{pmatrix} 40Q^2\beta^2 d_2 d_{10} + 54Q^2\beta^2 d_3 d_9 + 64Q^2\beta^2 d_4 d_8 + 70Q^2\beta^2 d_5 d_7 \\ +36Q^2\beta^2 d_6{}^2 + 40Q^2\beta d_1 d_{10} + 72Q^2\beta d_2 d_9 + 96Q^2\beta d_3 d_8 + 112Q^2\beta d_4 d_7 + 120Q^2\beta d_5 d_6 \\ +18Q^2 d_1 d_9 + 32Q^2 d_2 d_8 + 42Q^2 d_3 d_7 + 48Q^2 d_4 d_6 + 25Q^2 d_5{}^2 - 160c_0{}^2 d_2 d_{10} - 216c_0{}^2 d_3 d_9 \\ -256c_0{}^2 d_4 d_8 - 280c_0{}^2 d_5 d_7 - 144c_0{}^2 d_6{}^2 - 160c_0 c_1 d_1 d_{10} - 288c_0 c_1 d_2 d_9 - 384c_0 c_1 d_3 d_8 \\ -448c_0 c_1 d_4 d_7 - 480c_0 c_1 d_5 d_6 - 144c_0 c_2 d_1 d_9 - 256c_0 c_2 d_2 d_8 - 336c_0 c_2 d_3 d_7 - 384c_0 c_2 d_4 d_6 \\ -200c_0 c_2 d_5{}^2 - 128c_0 c_3 d_1 d_8 - 224c_0 c_3 d_2 d_7 - 288c_0 c_3 d_3 d_6 - 320c_0 c_3 d_4 d_5 - 112c_0 c_4 d_1 d_7 \\ -192c_0 c_4 d_2 d_6 - 240c_0 c_4 d_3 d_5 - 128c_0 c_4 d_4{}^2 - 96c_0 c_5 d_1 d_6 - 160c_0 c_5 d_2 d_5 - 192c_0 c_5 d_3 d_4 \\ -80c_0 c_6 d_1 d_5 - 128c_0 c_6 d_2 d_4 - 72c_0 c_6 d_3{}^2 - 64c_0 c_7 d_1 d_4 - 96c_0 c_7 d_2 d_3 - 48c_0 c_8 d_1 d_3 \\ -32c_0 c_8 d_2{}^2 - 32c_0 c_9 d_1 d_2 - 8c_0 c_{10} d_1{}^2 - 72c_1{}^2 d_1 d_9 - 128c_1{}^2 d_2 d_8 - 168c_1{}^2 d_3 d_7 - 192c_1{}^2 d_4 d_6 \\ -100c_1{}^2 d_5{}^2 - 128c_1 c_2 d_1 d_8 - 224c_1 c_2 d_2 d_7 - 288c_1 c_2 d_3 d_6 - 320c_1 c_2 d_4 d_5 - 112c_1 c_3 d_1 d_7 \\ -192c_1 c_3 d_2 d_6 - 240c_1 c_3 d_3 d_5 - 128c_1 c_3 d_4{}^2 - 96c_1 c_4 d_1 d_6 - 160c_1 c_4 d_2 d_5 - 192c_1 c_4 d_3 d_4 \\ -80c_1 c_5 d_1 d_5 - 128c_1 c_5 d_2 d_4 - 72c_1 c_5 d_3{}^2 - 64c_1 c_6 d_1 d_4 - 96c_1 c_6 d_2 d_3 - 48c_1 c_7 d_1 d_3 \\ -32c_1 c_7 d_2{}^2 - 32c_1 c_8 d_1 d_2 - 8c_1 c_9 d_1{}^2 - 56c_2{}^2 d_1 d_7 - 96c_2{}^2 d_2 d_6 - 120c_2{}^2 d_3 d_5 - 64c_2{}^2 d_4{}^2 \end{pmatrix}$$

$$-96c_2c_3d_1d_6-160c_2c_3d_2d_5-192c_2c_3d_3d_4-80c_2c_4d_1d_5-128c_2c_4d_2d_4-72c_2c_4{d_3}^2$$
$$-64c_2c_5d_1d_4-96c_2c_5d_2d_3-48c_2c_6d_1d_3-32c_2c_6{d_2}^2-32c_2c_7d_1d_2-8c_2c_8{d_1}^2-40{c_3}^2d_1d_5$$
$$-64{c_3}^2d_2d_4-36{c_3}^2{d_3}^2-64c_3c_4d_1d_4-96c_3c_4d_2d_3-48c_3c_5d_1d_3-32c_3c_5{d_2}^2-32c_3c_6d_1d_2 \quad ,$$
$$-8c_3c_7{d_1}^2-24{c_4}^2d_1d_3-16{c_4}^2{d_2}^2-32c_4c_5d_1d_2-8c_4c_6{d_1}^2-4{c_5}^2{d_1}^2)$$

$$c_{12}=-\frac{1}{264\beta^2(2\beta^2c_2-\beta\nu c_1+3\beta c_1-\nu c_0+c_0+1)}(1320\beta^4c_3c_{11}+2160\beta^4c_4c_{10}$$
$$+2880\beta^4c_5c_9+3360\beta^4c_6c_8-660\beta^3\nu c_3c_{10}-924\beta^3\nu c_6c_7+3212\beta^3c_2c_{11}+6300\beta^3c_3c_{10}$$
$$+11600\beta^3c_5c_8+12852\beta^3c_6c_7-1356\beta^2\nu {c_6}^2+2398\beta^2c_1c_{11}+6304\beta^2c_2c_{10}$$
$$+10686\beta^2c_3c_9+14536\beta^2c_4c_8+17134\beta^2c_5c_7-506\beta\nu c_0c_{11}-1206\beta\nu c_1c_{10}+506\beta c_0c_{11}$$
$$+2406\beta c_1c_{10}+5078\beta c_2c_9+9858\beta c_4c_7-240\nu c_0c_{10}+240c_{10}-484\beta^3\nu c_2c_{11}$$
$$-880\beta^3\nu c_5c_8+9288\beta^3c_4c_9-1012\beta^2\nu c_1c_{11}-1624\beta^2\nu c_2c_{10}-2100\beta^2\nu c_3c_9 \quad ,$$
$$-2440\beta^2\nu c_4c_8-2644\beta^2\nu c_5c_7-1766\beta\nu c_2c_9-2186\beta\nu c_3c_8-2466\beta\nu c_4c_7$$
$$-2606\beta\nu c_5c_6+7754\beta c_3c_8+11006\beta c_5c_6-456\nu c_1c_9-624\nu c_2c_8-744\nu c_3c_7-816\nu c_4c_6$$
$$+36{d_6}^2-792\beta^3\nu c_4c_9+1295{c_5}^2+1764\beta^4{c_7}^2+506\beta c_{11}+9024\beta^2{c_6}^2-420\nu {c_5}^2$$
$$+240c_0c_{10}+798c_1c_9+1456c_2c_8+2046c_3c_7+2448c_4c_6+22d_1d_{11}+40d_2d_{10}+54d_3d_9$$
$$+64d_4d_8+70d_5d_7)$$

$$d_{12}=-\frac{1}{6d_1(Q^2\beta^2-4{c_0}^2)}(11\,Q^2\beta^2d_2d_{11}+15Q^2\beta^2d_3d_{10}+18Q^2\beta^2d_4d_9+20Q^2\beta^2d_5d_8$$
$$+21Q^2\beta^2d_6d_7+11Q^2\beta d_1d_{11}+20Q^2\beta d_2d_{10}+27Q^2\beta d_3d_9+32Q^2\beta d_4d_8+35Q^2\beta d_5d_7$$
$$+18Q^2\beta {d_6}^2+5Q^2d_1d_{10}+9Q^2d_2d_9+12Q^2d_3d_8+14Q^2d_4d_7+15Q^2d_5d_6-44{c_0}^2d_2d_{11}$$
$$-60{c_0}^2d_3d_{10}-72{c_0}^2d_4d_9-80{c_0}^2d_5d_8-84{c_0}^2d_6d_7-44c_0c_1d_1d_{11}-80c_0c_1d_2d_{10}$$
$$-108c_0c_1d_3d_9-128c_0c_1d_4d_8-140c_0c_1d_5d_7-72c_0c_1{d_6}^2-40c_0c_2d_1d_{10}-72c_0c_2d_2d_9$$
$$-96c_0c_2d_3d_8-112c_0c_2d_4d_7-120c_0c_2d_5d_6-36c_0c_3d_1d_9-64c_0c_3d_2d_8-84c_0c_3d_3d_7$$
$$-96c_0c_3d_4d_6-50c_0c_3{d_5}^2-32c_0c_4d_1d_8-56c_0c_4d_2d_7-72c_0c_4d_3d_6-80c_0c_4d_4d_5$$
$$-28c_0c_5d_1d_7-48c_0c_5d_2d_6-60c_0c_5d_3d_5-32c_0c_5{d_4}^2-24c_0c_6d_1d_6-40c_0c_6d_2d_5$$
$$-48c_0c_6d_3d_4-20c_0c_7d_1d_5-32c_0c_7d_2d_4-18c_0c_7{d_3}^2-16c_0c_8d_1d_4-24c_0c_8d_2d_3$$
$$-12c_0c_9d_1d_3-8c_0c_9{d_2}^2-8c_0c_{10}d_1d_2-2c_0c_{11}{d_1}^2-20{c_1}^2d_1d_{10}-36{c_1}^2d_2d_9-48{c_1}^2d_3d_8$$
$$-56{c_1}^2d_4d_7-60{c_1}^2d_5d_6-36c_1c_2d_1d_9-64c_1c_2d_2d_8-84c_1c_2d_3d_7-96c_1c_2d_4d_6 \quad ,$$
$$-50c_1c_2{d_5}^2-32c_1c_3d_1d_8-56c_1c_3d_2d_7-72c_1c_3d_3d_6-80c_1c_3d_4d_5-28c_1c_4d_1d_7$$
$$-48c_1c_4d_2d_6-60c_1c_4d_3d_5-32c_1c_4{d_4}^2-24c_1c_5d_1d_6-40c_1c_5d_2d_5-48c_1c_5d_3d_4$$
$$-20c_1c_6d_1d_5-32c_1c_6d_2d_4-18c_1c_6{d_3}^2-16c_1c_7d_1d_4-24c_1c_7d_2d_3-12c_1c_8d_1d_3$$
$$-8c_1c_8{d_2}^2-8c_1c_9d_1d_2-2c_1c_{10}{d_1}^2-16{c_2}^2d_1d_8-28{c_2}^2d_2d_7-36{c_2}^2d_3d_6-40{c_2}^2d_4d_5$$
$$-28c_2c_3d_1d_7-48c_2c_3d_2d_6-60c_2c_3d_3d_5-32c_2c_3{d_4}^2-24c_2c_4d_1d_6-40c_2c_4d_2d_5$$
$$-48c_2c_4d_3d_4-20c_2c_5d_1d_5-32c_2c_5d_2d_4-18c_2c_5{d_3}^2-16c_2c_6d_1d_4-24c_2c_6d_2d_3$$
$$-12c_2c_7d_1d_3-8c_2c_7{d_2}^2-8c_2c_8d_1d_2-2c_2c_9{d_1}^2-12{c_3}^2d_1d_6-20{c_3}^2d_2d_5-24{c_3}^2d_3d_4$$
$$-20c_3c_4d_1d_5-32c_3c_4d_2d_4-18c_3c_4{d_3}^2-16c_3c_5d_1d_4-24c_3c_5d_2d_3-12c_3c_6d_1d_3$$
$$-8c_3c_6{d_2}^2-8c_3c_7d_1d_2-2c_3c_8{d_1}^2-8{c_4}^2d_1d_4-12{c_4}^2d_2d_3-12c_4c_5d_1d_3-8c_4c_5{d_2}^2$$
$$-8c_4c_6d_1d_2-2c_4c_7{d_1}^2-4{c_5}^2d_1d_2-2c_5c_6{d_1}^2)$$

$$
\begin{aligned}
c_{13} = &-\tfrac{1}{156\beta^2(2\beta^2c_2-\beta\nu c_1+3\beta c_1-\nu c_0+c_0+1)}(792\beta^4c_3c_{12}+1320\beta^4c_4c_{11}\\
&+1800\beta^4c_5c_{10}+2160\beta^4c_6c_9+2352\beta^4c_7c_8+1920\beta^3c_2c_{12}+3828\beta^3c_3c_{11}-970\beta^2\nu c_2c_{11}\\
&+1428\beta^2c_1c_{12}+3808\beta^2c_2c_{11}+6576\beta^2c_3c_{10}+9156\beta^2c_4c_9+11116\beta^2c_5c_8+12168\beta^2c_6c_7\\
&-1060\beta\nu c_2c_{10}-834\beta\nu c_6{}^2+300\beta c_0c_{12}+1444\beta c_1c_{11}+3100\beta c_2c_{10}+4836\beta c_3c_9\\
&+143c_{11}-288\beta^3\nu c_2c_{12}-396\beta^3\nu c_3c_{11}-576\beta^3\nu c_6c_8-294\beta^3\nu c_7{}^2+5760\beta^3c_4c_{10}\\
&+7380\beta^3c_5c_9+8448\beta^3c_6c_8-600\beta^2\nu c_1c_{12}-1488\beta^2\nu c_4c_9-300\beta\nu c_0c_{12}-1630\beta\nu c_5c_7\\
&+6316\beta c_4c_8+7300\beta c_5c_7-143\nu c_0c_{11}-273\nu c_1c_{10}-377\nu c_2c_9-455\nu c_3c_8-533\nu c_5c_6\\
&-480\beta^3\nu c_4c_{10}-540\beta^3\nu c_5c_9+4410\beta^3c_7{}^2-1266\beta^2\nu c_3c_{10}-1636\beta^2\nu c_5c_8-1710\beta^2\nu c_6c_7\\
&-718\beta\nu c_1c_{11}-1326\beta\nu c_3c_9-1516\beta\nu c_4c_8+3822\beta c_6{}^2-507\nu c_4c_7+300\beta c_{12}+143c_0c_{11}\\
&+483c_1c_{10}+899c_2c_9+1295c_3c_8+1599c_4c_7+1763c_5c_6+12d_1d_{12}+22d_2d_{11}+30d_3d_{10}\\
&+36d_4d_9+40d_5d_8+42d_6d_7)
\end{aligned}
,
$$

$$
\begin{aligned}
d_{13} = &-\tfrac{1}{26d_1(Q^2\beta^2-4c_0{}^2)}(48\,Q^2\beta^2d_2d_{12}+66Q^2\beta^2d_3d_{11}+80Q^2\beta^2d_4d_{10}\\
&+90Q^2\beta^2d_5d_9+96Q^2\beta^2d_6d_8+49Q^2\beta^2d_7{}^2+48Q^2\beta d_1d_{12}+88Q^2\beta d_2d_{11}+120Q^2\beta d_3d_{10}\\
&+144Q^2\beta d_4d_9+160Q^2\beta d_5d_8+168Q^2\beta d_6d_7+22Q^2d_1d_{11}+40Q^2d_2d_{10}+54Q^2d_3d_9\\
&+64Q^2d_4d_8+70Q^2d_5d_7+36Q^2d_6{}^2-192c_0{}^2d_2d_{12}-264c_0{}^2d_3d_{11}-320c_0{}^2d_4d_{10}\\
&-360c_0{}^2d_5d_9-384c_0{}^2d_6d_8-196c_0{}^2d_7{}^2-192c_0c_1d_1d_{12}-352c_0c_1d_2d_{11}-480c_0c_1d_3d_{10}\\
&-576c_0c_1d_4d_9-640c_0c_1d_5d_8-672c_0c_1d_6d_7-176c_0c_2d_1d_{11}-320c_0c_2d_2d_{10}-432c_0c_2d_3d_9\\
&-512c_0c_2d_4d_8-560c_0c_2d_5d_7-288c_0c_2d_6{}^2-160c_0c_3d_1d_{10}-288c_0c_3d_2d_9-384c_0c_3d_3d_8\\
&-448c_0c_3d_4d_7-480c_0c_3d_5d_6-144c_0c_4d_1d_9-256c_0c_4d_2d_8-336c_0c_4d_3d_7-384c_0c_4d_4d_6\\
&-200c_0c_4d_5{}^2-128c_0c_5d_1d_8-224c_0c_5d_2d_7-288c_0c_5d_3d_6-320c_0c_5d_4d_5-112c_0c_6d_1d_7\\
&-192c_0c_6d_2d_6-240c_0c_6d_3d_5-128c_0c_6d_4{}^2-96c_0c_7d_1d_6-160c_0c_7d_2d_5-192c_0c_7d_3d_4\\
&-80c_0c_8d_1d_5-128c_0c_8d_2d_4-72c_0c_8d_3{}^2-64c_0c_9d_1d_4-96c_0c_9d_2d_3-48c_0c_{10}d_1d_3\\
&-32c_0c_{10}d_2{}^2-32c_0c_{11}d_1d_2-8c_0c_{12}d_1{}^2-88c_1{}^2d_1d_{11}-160c_1{}^2d_2d_{10}-216c_1{}^2d_3d_9-256c_1{}^2d_4d_8\\
&-280c_1{}^2d_5d_7-144c_1{}^2d_6{}^2-160c_1c_2d_1d_{10}-288c_1c_2d_2d_9-384c_1c_2d_3d_8-448c_1c_2d_4d_7\\
&-480c_1c_2d_5d_6-144c_1c_3d_1d_9-256c_1c_3d_2d_8-336c_1c_3d_3d_7-384c_1c_3d_4d_6-200c_1c_3d_5{}^2\\
&-128c_1c_4d_1d_8-224c_1c_4d_2d_7-288c_1c_4d_3d_6-320c_1c_4d_4d_5-112c_1c_5d_1d_7-192c_1c_5d_2d_6\\
&-240c_1c_5d_3d_5-128c_1c_5d_4{}^2-96c_1c_6d_1d_6-160c_1c_6d_2d_5-192c_1c_6d_3d_4-80c_1c_7d_1d_5\\
&-128c_1c_7d_2d_4-72c_1c_7d_3{}^2-64c_1c_8d_1d_4-96c_1c_8d_2d_3-48c_1c_9d_1d_3-32c_1c_9d_2{}^2\\
&-32c_1c_{10}d_1d_2-8c_1c_{11}d_1{}^2-72c_2{}^2d_1d_9-128c_2{}^2d_2d_8-168c_2{}^2d_3d_7-192c_2{}^2d_4d_6\\
&-100c_2{}^2d_5{}^2-128c_2c_3d_1d_8-224c_2c_3d_2d_7-288c_2c_3d_3d_6-320c_2c_3d_4d_5-112c_2c_4d_1d_7\\
&-192c_2c_4d_2d_6-240c_2c_4d_3d_5-128c_2c_4d_4{}^2-96c_2c_5d_1d_6-160c_2c_5d_2d_5-192c_2c_5d_3d_4\\
&-80c_2c_6d_1d_5-128c_2c_6d_2d_4-72c_2c_6d_3{}^2-64c_2c_7d_1d_4-96c_2c_7d_2d_3-48c_2c_8d_1d_3\\
&-32c_2c_8d_2{}^2-32c_2c_9d_1d_2-8c_2c_{10}d_1{}^2-56c_3{}^2d_1d_7-96c_3{}^2d_2d_6-120c_3{}^2d_3d_5-64c_3{}^2d_4{}^2\\
&-96c_3c_4d_1d_6-160c_3c_4d_2d_5-192c_3c_4d_3d_4-80c_3c_5d_1d_5-128c_3c_5d_2d_4-72c_3c_5d_3{}^2\\
&-64c_3c_6d_1d_4-96c_3c_6d_2d_3-48c_3c_7d_1d_3-32c_3c_7d_2{}^2-32c_3c_8d_1d_2-8c_3c_9d_1{}^2-40c_4{}^2d_1d_5\\
&-64c_4{}^2d_2d_4-36c_4{}^2d_3{}^2-64c_4c_5d_1d_4-96c_4c_5d_2d_3-48c_4c_6d_1d_3-32c_4c_6d_2{}^2-32c_4c_7d_1d_2\\
&-8c_4c_8d_1{}^2-24c_5{}^2d_1d_3-16c_5{}^2d_2{}^2-32c_5c_6d_1d_2-8c_5c_7d_1{}^2-4c_6{}^2d_1{}^2)
\end{aligned}
,
$$

$$c_{14} = -\frac{1}{364\beta^2(2\beta^2c_2-\beta\nu c_1+3\beta c_1-\nu c_0+c_0+1)}(-676\beta^3\nu c_2c_{13} - 936\beta^3\nu c_3c_{12}$$
$$-1144\beta^3\nu c_4c_{11} - 1300\beta^3\nu c_5c_{10} - 1404\beta^3\nu c_6c_9 - 1456\beta^3\nu c_7c_8 - 1404\beta^2\nu c_1c_{13}$$
$$-2284\beta^2\nu c_2c_{12} - 3004\beta^2\nu c_3c_{11} - 3564\beta^2\nu c_4c_{10} - 3964\beta^2\nu c_5c_9 - 4204\beta^2\nu c_6c_8$$
$$-2506\beta\nu c_2c_{11} - 3162\beta\nu c_3c_{10} - 3654\beta\nu c_4c_9 - 3982\beta\nu c_5c_8 - 4146\beta\nu c_6c_7$$
$$-1872\beta^4c_3c_{13} + 3168\beta^4c_4c_{12} + 4400\beta^4c_5c_{11} + 5400\beta^4c_6c_{10} + 6048\beta^4c_7c_9$$
$$+16401\beta^2{c_7}^2 - 702\beta\nu c_0c_{13} - 1686\beta\nu c_1c_{12} + 3414\beta c_1c_{12} + 7434\beta c_2c_{11} + 11802\beta c_3c_{10}$$
$$+15750\beta c_4c_9 + 18702\beta c_5c_8 - 336\nu c_0c_{12} - 644\nu c_1c_{11} - 896\nu c_2c_{10} - 1092\nu c_3c_9 \qquad ,$$
$$-1232\nu c_4c_8 - 1316\nu c_5c_7 + 336c_0c_{12} + 1150c_1c_{11} + 2176c_2c_{10} + 3198c_3c_9 + 4048c_4c_8$$
$$+4606c_5c_7 + 23184\beta^3c_7c_8 + 3354\beta^2c_1c_{13} + 9052\beta^2c_2c_{12} + 15874\beta^2c_3c_{11} + 22524\beta^2c_4c_{10}$$
$$+27994\beta^2c_5c_9 + 31564\beta^2c_6c_8 + 702\beta c_0c_{13} + 20274\beta c_6c_7 - 672\nu{c_6}^2 + 702\beta c_{13} + 26d_1d_{13}$$
$$+48d_2d_{12} + 66d_3d_{11} + 80d_4d_{10} + 3136\beta^4{c_8}^2 + 4524\beta^3c_2c_{13} + 9144\beta^3c_3c_{12} + 13992\beta^3c_4c_{11}$$
$$+18300\beta^3c_5c_{10} + 21492\beta^3c_6c_9 - 2142\beta^2\nu{c_7}^2 + 2400{c_6}^2 + 90d_5d_9 + 96d_6d_8 + 49{d_7}^2$$
$$+336c_{12})$$

$$d_{14} = -\frac{1}{14d_1(Q^2\beta^2-4{c_0}^2)}(26Q^2\beta^2d_2d_{13} + 36Q^2\beta^2d_3d_{12} + 44Q^2\beta^2d_4d_{11}$$
$$+50Q^2\beta^2d_5d_{10} + 54Q^2\beta^2d_6d_9 + 56Q^2\beta^2d_7d_8 + 26Q^2\beta d_1d_{13} + 48Q^2\beta d_2d_{12} + 66Q^2\beta d_3d_{11}$$
$$+80Q^2\beta d_4d_{10} + 90Q^2\beta d_5d_9 + 96Q^2\beta d_6d_8 + 49Q^2\beta{d_7}^2 + 12Q^2d_1d_{12} + 22Q^2d_2d_{11}$$
$$+30Q^2d_3d_{10} + 36Q^2d_4d_9 + 40Q^2d_5d_8 + 42Q^2d_6d_7 - 104{c_0}^2d_2d_{13} - 144{c_0}^2d_3d_{12}$$
$$-176{c_0}^2d_4d_{11} - 200{c_0}^2d_5d_{10} - 216{c_0}^2d_6d_9 - 224{c_0}^2d_7d_8 - 104c_0c_1d_1d_{13} - 192c_0c_1d_2d_{12}$$
$$-264c_0c_1d_3d_{11} - 320c_0c_1d_4d_{10} - 360c_0c_1d_5d_9 - 384c_0c_1d_6d_8 - 196c_0c_1{d_7}^2 - 96c_0c_2d_1d_{12}$$
$$-176c_0c_2d_2d_{11} - 240c_0c_2d_3d_{10} - 288c_0c_2d_4d_9 - 320c_0c_2d_5d_8 - 336c_0c_2d_6d_7 - 88c_0c_3d_1d_{11}$$
$$-160c_0c_3d_2d_{10} - 216c_0c_3d_3d_9 - 256c_0c_3d_4d_8 - 280c_0c_3d_5d_7 - 144c_0c_3{d_6}^2 - 80c_0c_4d_1d_{10}$$
$$-144c_0c_4d_2d_9 - 192c_0c_4d_3d_8 - 224c_0c_4d_4d_7 - 240c_0c_4d_5d_6 - 72c_0c_5d_1d_9 - 128c_0c_5d_2d_8$$
$$-168c_0c_5d_3d_7 - 192c_0c_5d_4d_6 - 100c_0c_5{d_5}^2 - 64c_0c_6d_1d_8 - 112c_0c_6d_2d_7 - 144c_0c_6d_3d_6$$
$$-160c_0c_6d_4d_5 - 56c_0c_7d_1d_7 - 96c_0c_7d_2d_6 - 120c_0c_7d_3d_5 - 64c_0c_7{d_4}^2 - 48c_0c_8d_1d_6$$
$$-80c_0c_8d_2d_5 - 96c_0c_8d_3d_4 - 40c_0c_9d_1d_5 - 64c_0c_9d_2d_4 - 36c_0c_9{d_3}^2 - 32c_0c_{10}d_1d_4$$
$$-48c_0c_{10}d_2d_3 - 24c_0c_{11}d_1d_3 - 16c_0c_{11}{d_2}^2 - 16c_0c_{12}d_1d_2 - 4c_0c_{13}{d_1}^2 - 48{c_1}^2d_1d_{12} \qquad ,$$
$$-88{c_1}^2d_2d_{11} - 120{c_1}^2d_3d_{10} - 144{c_1}^2d_4d_9 - 160{c_1}^2d_5d_8 - 168{c_1}^2d_6d_7 - 88c_1c_2d_1d_{11}$$
$$-160c_1c_2d_2d_{10} - 216c_1c_2d_3d_9 - 256c_1c_2d_4d_8 - 280c_1c_2d_5d_7 - 144c_1c_2{d_6}^2 - 80c_1c_3d_1d_{10}$$
$$-144c_1c_3d_2d_9 - 192c_1c_3d_3d_8 - 224c_1c_3d_4d_7 - 240c_1c_3d_5d_6 - 72c_1c_4d_1d_9 - 128c_1c_4d_2d_8$$
$$-168c_1c_4d_3d_7 - 192c_1c_4d_4d_6 - 100c_1c_4{d_5}^2 - 64c_1c_5d_1d_8 - 112c_1c_5d_2d_7 - 144c_1c_5d_3d_6$$
$$-160c_1c_5d_4d_5 - 56c_1c_6d_1d_7 - 96c_1c_6d_2d_6 - 120c_1c_6d_3d_5 - 64c_1c_6{d_4}^2 - 48c_1c_7d_1d_6$$
$$-80c_1c_7d_2d_5 - 96c_1c_7d_3d_4 - 40c_1c_8d_1d_5 - 64c_1c_8d_2d_4 - 36c_1c_8{d_3}^2 - 32c_1c_9d_1d_4$$
$$-48c_1c_9d_2d_3 - 24c_1c_{10}d_1d_3 - 16c_1c_{10}{d_2}^2 - 16c_1c_{11}d_1d_2 - 4c_1c_{12}{d_1}^2 - 40{c_2}^2d_1d_{10}$$
$$-72{c_2}^2d_2d_9 - 96{c_2}^2d_3d_8 - 112{c_2}^2d_4d_7 - 120{c_2}^2d_5d_6 - 72c_2c_3d_1d_9 - 128c_2c_3d_2d_8$$
$$-168c_2c_3d_3d_7 - 192c_2c_3d_4d_6 - 100c_2c_3{d_5}^2 - 64c_2c_4d_1d_8 - 112c_2c_4d_2d_7 - 144c_2c_4d_3d_6$$
$$-160c_2c_4d_4d_5 - 56c_2c_5d_1d_7 - 96c_2c_5d_2d_6 - 120c_2c_5d_3d_5 - 64c_2c_5{d_4}^2 - 48c_2c_6d_1d_6$$
$$-80c_2c_6d_2d_5 - 96c_2c_6d_3d_4 - 40c_2c_7d_1d_5 - 64c_2c_7d_2d_4 - 36c_2c_7{d_3}^2 - 32c_2c_8d_1d_4$$
$$-48c_2c_8d_2d_3 - 24c_2c_9d_1d_3 - 16c_2c_9{d_2}^2 - 16c_2c_{10}d_1d_2 - 4c_2c_{11}{d_1}^2 - 32{c_3}^2d_1d_8 - 56{c_3}^2d_2d_7$$

$$
\begin{aligned}
&-72c_3{}^2d_3d_6-80c_3{}^2d_4d_5-56c_3c_4d_1d_7-96c_3c_4d_2d_6-120c_3c_4d_3d_5-64c_3c_4d_4{}^2-48c_3c_5d_1d_6\\
&-80c_3c_5d_2d_5-96c_3c_5d_3d_4-40c_3c_6d_1d_5-64c_3c_6d_2d_4-36c_3c_6d_3{}^2-32c_3c_7d_1d_4\\
&-48c_3c_7d_2d_3-24c_3c_8d_1d_3-16c_3c_8d_2{}^2-16c_3c_9d_1d_2-4c_3c_{10}d_1{}^2-24c_4{}^2d_1d_6-40c_4{}^2d_2d_5\\
&-48c_4{}^2d_3d_4-40c_4c_5d_1d_5-64c_4c_5d_2d_4-36c_4c_5d_3{}^2-32c_4c_6d_1d_4-48c_4c_6d_2d_3-24c_4c_7d_1d_3\\
&-16c_4c_7d_2{}^2-16c_4c_8d_1d_2-4c_4c_9d_1{}^2-16c_5{}^2d_1d_4-24c_5{}^2d_2d_3-24c_5c_6d_1d_3-16c_5c_6d_2{}^2\\
&-16c_5c_7d_1d_2-4c_5c_8d_1{}^2-8c_6{}^2d_1d_2-4c_6c_7d_1{}^2)
\end{aligned},
$$

$$
\begin{aligned}
&c_{15}=-\frac{1}{210\beta^2(2\beta^2c_2-\beta\nu c_1+3\beta c_1-\nu c_0+c_0+1)}(2632\beta^3c_2c_{14}+8352\beta^3c_4c_{12}\\
&+11110\beta^3c_5c_{11}+13320\beta^3c_6c_{10}+14742\beta^3c_7c_9-1758\beta^2\nu c_3c_{12}-2102\beta^2\nu c_4c_{11}\\
&-2360\beta^2\nu c_5c_{10}-2532\beta^2\nu c_6c_9-2618\beta^2\nu c_7c_8-406\beta\nu c_0c_{14}-978\beta\nu c_1c_{13}+6720\beta c_7{}^2\\
&+406\beta c_{14}+195c_0c_{13}+675c_1c_{12}+1295c_2c_{11}+1935c_3c_{10}+2499c_4c_9+2915c_5c_8+3135c_6c_7\\
&+26d_2d_{13}+36d_3d_{12}+44d_4d_{11}+195c_{13}+1872\beta^4c_4c_{13}-448\beta^3\nu c_8{}^2+5382\beta^3c_3c_{13}\\
&+13586\beta^2c_4c_{11}+406\beta c_0c_{14}+1992\beta c_1c_{13}+4390\beta c_2c_{12}+7072\beta c_3c_{11}+9606\beta c_4c_{10}\\
&+11656\beta c_5c_9+12982\beta c_6c_8-195\nu c_0c_{13}-375\nu c_1c_{12}-525\nu c_2c_{11}-645\nu c_3c_{10}-735\nu c_4c_9\\
&-795\nu c_5c_8-825\nu c_6c_7-1281\beta\nu c_7{}^2+9426\beta^2c_3c_{12}+1946\beta^2c_1c_{14}+19866\beta^2c_6c_9\\
&+17210\beta^2c_5c_{10}+5306\beta^2c_2c_{13}+21266\beta^2c_7c_8+4032\beta^4c_8c_9+2640\beta^4c_5c_{12}+3780\beta^4c_7c_{10}\\
&+3300\beta^4c_6c_{11}+1092\beta^4c_3c_{14}-1328\beta^2\nu c_2c_{13}-812\beta^2\nu c_1c_{14}+14d_1d_{14}+7616\beta^3c_8{}^2+50d_5d_{10}\\
&+54d_6d_9+56d_7d_8-392\beta^3\nu c_2c_{14}-546\beta^3\nu c_3c_{13}-672\beta^3\nu c_4c_{12}-770\beta^3\nu c_5c_{11}-840\beta^3\nu c_6c_{10}\\
&-882\beta^3\nu c_7c_9-1462\beta\nu c_2c_{12}-1858\beta\nu c_3c_{11}-2166\beta\nu c_4c_{10}-2386\beta\nu c_5c_9-2518\beta\nu c_6c_8)
\end{aligned},
$$

$$
\begin{aligned}
&d_{15}=-\frac{1}{30d_1(Q^2\beta^2-4c_0{}^2)}(120Q^2\beta^2d_6d_{10}+104Q^2\beta d_2d_{13}-336c_0c_6d_3d_7-128c_0c_7d_1d_8\\
&-192c_0c_9d_3d_4-128c_0c_{10}d_2d_4-64c_0c_{11}d_1d_4-96c_0c_{11}d_2d_3-176c_1c_3d_1d_{11}-384c_1c_4d_3d_8\\
&-128c_1c_7d_4{}^2-192c_1c_8d_3d_4-72c_1c_9d_3{}^2-160c_2{}^2d_2d_{10}-216c_2{}^2d_3d_9-256c_2{}^2d_4d_8\\
&-64c_4c_7d_1d_4-8c_4c_{10}d_1{}^2-40c_5{}^2d_1d_5-64c_5{}^2d_2d_4-8c_5c_9d_1{}^2-4c_7{}^2d_1{}^2+96Q^2\beta^2d_4d_{12}\\
&-312c_0{}^2d_3d_{13}-440c_0{}^2d_5d_{11}-504c_0{}^2d_7d_9-224c_0c_1d_1d_{14}-352c_0c_3d_2d_{11}-448c_0c_5d_4d_7\\
&-256c_0c_6d_2d_8-352c_1c_2d_2d_{11}-512c_1c_3d_4d_8-32c_1c_{11}d_2{}^2-8c_1c_{13}d_1{}^2-88c_2{}^2d_1d_{11}\\
&-280c_2{}^2d_5d_7-200c_2c_4d_5{}^2-128c_2c_6d_4{}^2-224c_3c_4d_2d_7-160c_3c_6d_2d_5-32c_3c_{10}d_1d_2\\
&-32c_4c_9d_1d_2-48c_5c_7d_1d_3+200Q^2\beta d_5d_{10}-160c_0c_5d_1d_{10}-480c_0c_5d_5d_6-128c_0c_8d_4{}^2\\
&-72c_0c_{10}d_3{}^2-384c_1{}^2d_6d_8-288c_1c_4d_2d_9-480c_1c_4d_5d_6-144c_1c_5d_1d_9-160c_1c_8d_2d_5\\
&-80c_1c_9d_1d_5-128c_1c_9d_2d_4-64c_2c_9d_1d_4-8c_2c_{12}d_1{}^2-128c_3{}^2d_2d_8-128c_3c_4d_1d_8\\
&-240c_3c_5d_3d_5-64c_4{}^2d_4{}^2-192c_4c_5d_3d_4-36c_5{}^2d_3{}^2-16c_6{}^2d_2{}^2+176Q^2\beta d_4d_{11}\\
&-224c_0{}^2d_2d_{14}-480c_0{}^2d_6d_{10}-192c_0c_3d_1d_{12}-512c_0c_4d_4d_8-288c_0c_5d_2d_9-384c_0c_6d_4d_6\\
&-320c_0c_7d_4d_5-192c_1{}^2d_2d_{12}-264c_1{}^2d_3d_{11}-320c_1c_3d_2d_{10}-448c_1c_4d_4d_7-32c_2c_{11}d_1d_2\\
&-96c_3c_6d_1d_6-32c_3c_9d_2{}^2-56c_4{}^2d_1d_7-96c_4{}^2d_2d_6-96c_4c_5d_1d_6-48c_4c_8d_1d_3-32c_4c_8d_2{}^2\\
&-96c_5c_6d_2d_3+56Q^2\beta d_1d_{14}+144Q^2\beta d_3d_{12}+224Q^2\beta d_7d_8-320c_0c_4d_2d_{10}-288c_0c_4d_6{}^2\\
&-384c_0c_5d_3d_8-200c_0c_6d_5{}^2-112c_0c_8d_1d_7-240c_0c_8d_3d_5-96c_0c_9d_1d_6-360c_1{}^2d_5d_9\\
&-192c_1c_2d_1d_{12}-640c_1c_2d_5d_8-64c_1c_{10}d_1d_4-144c_2{}^2d_6{}^2-112c_3c_5d_1d_7-192c_3c_5d_2d_6\\
&-80c_3c_7d_1d_5-160c_4c_5d_2d_5-80c_4c_6d_1d_5+110Q^2\beta^2d_5d_{11}+126Q^2\beta^2d_7d_9+49Q^2d_7{}^2\\
&-416c_0c_1d_2d_{13}-576c_0c_1d_3d_{12}-480c_0c_3d_3d_{10}-576c_0c_3d_4d_9-432c_0c_4d_3d_9-144c_0c_6d_1d_9\\
&-288c_0c_7d_3d_6-320c_1{}^2d_4d_{10}-196c_1{}^2d_7{}^2-672c_1c_2d_6d_7-288c_1c_3d_6{}^2-200c_1c_5d_5{}^2
\end{aligned}
$$

$$
\begin{aligned}
&-64c_3c_8d_1d_4-96c_3c_8d_2d_3-128c_4c_6d_2d_4-32c_5c_8d_1d_2-8c_6c_8{d_1}^2+64Q^2\beta^2{d_8}^2+26Q^2d_1d_{13}\\
&+48Q^2d_2d_{12}+66Q^2d_3d_{11}+80Q^2d_4d_{10}+90Q^2d_5d_9+96Q^2d_6d_8-384{c_0}^2d_4d_{12}-392c_0c_2{d_7}^2\\
&-640c_0c_3d_5d_8-224c_0c_7d_2d_7-192c_0c_8d_2d_6-48c_0c_{12}d_1d_3-32c_0c_{13}d_1d_2-432c_1c_3d_3d_9\\
&-160c_1c_4d_1d_{10}-288c_3c_4d_3d_6-48c_3c_9d_1d_3-96c_4c_7d_2d_3-32c_6c_7d_1d_2+78Q^2\beta^2d_3d_{13}\\
&-256{c_0}^2{d_8}^2-672c_0c_3d_6d_7-160c_0c_9d_2d_5-32c_0c_{12}{d_2}^2-8c_0c_{14}{d_1}^2-104{c_1}^2d_1d_{13}\\
&-480c_1c_2d_3d_{10}-576c_1c_2d_4d_9-560c_1c_3d_5d_7-96c_1c_8d_1d_6-192c_2c_7d_3d_4-80c_2c_8d_1d_5\\
&-128c_2c_8d_2d_4-72c_2c_8{d_3}^2-48c_2c_{10}d_1d_3-32c_2c_{10}{d_2}^2-100{c_3}^2{d_5}^2-192c_3c_6d_3d_4-120{c_4}^2d_3d_5\\
&-72c_4c_6{d_3}^2-704c_0c_1d_4d_{11}-800c_0c_1d_5d_{10}-864c_0c_1d_6d_9-896c_0c_1d_7d_8-208c_0c_2d_1d_{13}\\
&-384c_0c_2d_2d_{12}-528c_0c_2d_3d_{11}-640c_0c_2d_4d_{10}-720c_0c_2d_5d_9-768c_0c_2d_6d_8-224c_2c_5d_2d_7\\
&-288c_2c_5d_3d_6-320c_2c_5d_4d_5-112c_2c_6d_1d_7-192c_2c_6d_2d_6-240c_2c_6d_3d_5-96c_2c_7d_1d_6\\
&-160c_2c_7d_2d_5-288c_1c_6d_3d_6-320c_1c_6d_4d_5-112c_1c_7d_1d_7-192c_1c_7d_2d_6-240c_1c_7d_3d_5\\
&-96c_1c_{10}d_2d_3-48c_1c_{11}d_1d_3-32c_1c_{12}d_1d_2-160c_2c_3d_1d_{10}-288c_2c_3d_2d_9-384c_2c_3d_3d_8\\
&-448c_2c_3d_4d_7-480c_2c_3d_5d_6-144c_2c_4d_1d_9-256c_2c_4d_2d_8-336c_2c_4d_3d_7-384c_2c_4d_4d_6\\
&-128c_2c_5d_1d_8+56Q^2\beta^2d_2d_{14}+216Q^2\beta d_6d_9-176c_0c_4d_1d_{11}-560c_0c_4d_5d_7-80c_0c_{10}d_1d_5\\
&-256c_1c_5d_2d_8-336c_1c_5d_3d_7-384c_1c_5d_4d_6-128c_1c_6d_1d_8-224c_1c_6d_2d_7-96c_2c_9d_2d_3\\
&-72{c_3}^2d_1d_9-168{c_3}^2d_3d_7-192{c_3}^2d_4d_6-320c_3c_4d_4d_5-128c_3c_5{d_4}^2-128c_3c_7d_2d_4\\
&-72c_3c_7{d_3}^2-8c_3c_{11}{d_1}^2-64c_5c_6d_1d_4-32c_5c_7{d_2}^2-24{c_6}^2d_1d_3\big)
\end{aligned}
\quad .
$$

References

1. Delfani, M.R. Nonlinear elasticity of monolayer hexagonal crystals: Theory and application to circular bulge test. *Eur. J. Mech. A Solid.* **2018**, *68*, 117–132. [CrossRef]
2. Dai, Z.; Lu, N. Poking and bulging of suspended thin sheets: Slippage, instabilities, and metrology. *J. Mech. Phys. Solids* **2021**, *149*, 104320. [CrossRef]
3. Gutscher, G.; Wu, H.C.; Ngaile, G.; Altan, T. Determination of flow stress for sheet metal forming using the viscous pressure bulge (VPB) test. *J. Mater. Process. Technol.* **2004**, *146*, 1–7. [CrossRef]
4. Sun, J.Y.; Qian, S.H.; Li, Y.M.; He, X.T.; Zheng, Z.L. Theoretical study of adhesion energy measurement for film/substrate interface using pressurized blister test: Energy release rate. *Measurement* **2013**, *46*, 2278–2287. [CrossRef]
5. Ma, Y.; Wang, G.R.; Chen, Y.L.; Long, D.; Guan, Y.C.; Liu, L.Q.; Zhang, Z. Extended Hencky solution for the blister test of nanomembrane. *Extrem. Mech. Lett.* **2018**, *22*, 69–78. [CrossRef]
6. Cao, Z.; Tao, L.; Akinwande, D.; Huang, R.; Liechti, K.M. Mixed-mode traction-separation relations between graphene and copper by blister tests. *Int. J. Solids Struct.* **2016**, *84*, 147–159. [CrossRef]
7. Napolitanno, M.J.; Chudnovsky, A.; Moet, A. The constrained blister test for the energy of interfacial adhesion. *J. Adhes. Sci. Technol.* **1988**, *2*, 311–323. [CrossRef]
8. Pervier, M.L.A.; Hammond, D.W. Measurement of the fracture energy in mode I of atmospheric ice accreted on different materials using a blister test. *Eng. Fract. Mech.* **2019**, *214*, 223–232. [CrossRef]
9. Zhu, T.T.; Li, G.X.; Müftü, S.; Wan, K.T. Revisiting the constrained blister test to measure thin film adhesion. *J. Appl. Mech. T ASME* **2017**, *84*, 071005. [CrossRef]
10. Zhu, T.T.; Müftü, S.; Wan, K.T. One-dimensional constrained blister test to measure thin film adhesion. *J. Appl. Mech. T ASME* **2018**, *85*, 054501. [CrossRef]
11. Molla-Alipour, M.; Ganji, B.A. Analytical analysis of mems capacitive pressure sensor with circular diaphragm under dynamic load using differential transformation method (DTM). *Acta Mech. Solida Sin.* **2015**, *28*, 400–408. [CrossRef]
12. Lee, H.Y.; Choi, B. Theoretical and experimental investigation of the trapped air effect on air-sealed capacitive pressure sensor. *Sens. Actuators A* **2015**, *221*, 104–114. [CrossRef]
13. Mishra, R.B.; Khan, S.M.; Shaikh, S.F.; Hussain, A.M.; Hussain, M. Low-cost foil/paper based touch mode pressure sensing element as artificial skin module for prosthetic hand. In Proceedings of the 2020 3rd IEEE International Conference on Soft Robotics (RoboSoft), New Haven, CT, USA, 15 May–15 July 2020; pp. 194–200.
14. Meng, G.Q.; Ko, W.H. Modeling of circular diaphragm and spreadsheet solution programming for touch mode capacitive sensors. *Sens. Actuators A* **1999**, *75*, 45–52. [CrossRef]

15. Lian, Y.S.; Sun, J.Y.; Ge, X.M.; Yang, Z.X.; He, X.T.; Zheng, Z.L. A theoretical study of an improved capacitive pressure sensor: Closed-form solution of uniformly loaded annular membranes. *Measurement* **2017**, *111*, 84–92. [CrossRef]
16. Hencky, H. On the stress state in circular plates with vanishing bending stiffness. *Z. Angew. Math. Phys.* **1915**, *63*, 311–317.
17. Chien, W.Z. Asymptotic behavior of a thin clamped circular plate under uniform normal pressure at very large deflection. *Sci. Rep. Natl. Tsinghua Univ.* **1948**, *5*, 193–208.
18. Alekseev, S.A. Elastic circular membranes under the uniformly distributed loads. *Eng. Corpus* **1953**, *14*, 196–198.
19. Huang, P.F.; Song, Y.P.; Li, Q.; Liu, X.Q.; Feng, Y.Q. A theoretical study of circular orthotropic membrane under concentrated load: The relation of load and deflection. *IEEE Access* **2020**, *8*, 126127–126137. [CrossRef]
20. Rao, Y.; Qiao, S.; Dai, Z.; Lu, N. Elastic wetting: Substrate-supported droplets confined by soft elastic membranes. *J. Mech. Phys. Solids* **2021**, *151*, 104399. [CrossRef]
21. Chen, S.L.; Zheng, Z.L. Large deformation of circular membrane under the concentrated force. *Appl. Math. Mech.* **2003**, *24*, 25–28.
22. Chien, W.Z.; Wang, Z.Z.; Xu, Y.G.; Chen, S.L. The symmetrical deformation of circular membrane under the action of uniformly distributed loads in its central portion. *Appl. Math. Mech.* **1981**, *2*, 599–612.
23. Lian, Y.S.; Sun, J.Y.; Zhao, Z.H.; He, X.T.; Zheng, Z.L. A revisit of the boundary value problem for Föppl–Hencky membranes: Improvement of geometric equations. *Mathematics* **2020**, *8*, 631. [CrossRef]
24. Campbell, J.D. On the theory of initially tensioned circular membranes subjected to uniform pressure. *Q. J. Mech. Appl. Math.* **1956**, *9*, 84–93. [CrossRef]
25. Fichter, W.B. *Some Solutions for the Large Deflections of Uniformly Loaded Circular Membranes*; NASA: Washington, DC, USA, 1997; TP-3658.
26. Alekseev, S.A. Elastic annular membranes with a stiff centre under the concentrated force. *Eng. Corpus* **1951**, *10*, 71–80.
27. Sun, J.Y.; Zhang, Q.; Li, X.; He, X.T. Axisymmetric large deflection elastic analysis of hollow annular membranes under transverse uniform loading. *Symmetry* **2021**, *13*, 1770. [CrossRef]
28. Sun, J.Y.; Hu, J.L.; He, X.T.; Zheng, Z.L. A theoretical study of a clamped punch-loaded blister configuration: The quantitative relation of load and deflection. *Int. J. Mech. Sci.* **2010**, *52*, 928–936. [CrossRef]
29. Yang, Z.X.; Sun, J.Y.; Zhao, Z.H.; Li, S.Z.; He, X.T. A closed-form solution of prestressed annular membrane internally-connected with rigid circular plate and transversely-loaded by central shaft. *Mathematics* **2020**, *8*, 521. [CrossRef]